Reverse telescoping in a distal skarn system (Campiglia Marittima, Italy)

Simone Vezzoni*, Dipartimento di Scienze della Terra, Università di Pisa, Via Santa Maria 56 (56126), Pisa, Italy

Andrea Dini, Istituto di Geoscienze e Georisorse, CNR, Via Moruzzi 1 (56124), Pisa, Italy

Sergio Rocchi, Dipartimento di Scienze della Terra, Università di Pisa, Via Santa Maria 56 (56126), Pisa, Italy

*corresponding author: e-mail, vezzoni@dst.unipi.it

Keywords

Campiglia Marittima, distal skarn, magmatic rocks, ores, reverse telescoping

Abstract

The Campiglia Marittima Fe-Cu-Zn-Pb(-Ag) skarn deposit has long been regarded as a reference example of an exoskarn showing a symmetric outward mineralogical zoning of both skarn and ore minerals with respect to an axial mafic porphyry dike. Detailed field and underground mapping, along with three-dimensional reconstruction of the geometries of skarn and magmatic bodies, integrated with new petrographic, mineralogical and geochemical data, argue against this model. The shapes of the skarn bodies and the growth versors of skarn minerals in particular, are ascribed to the focusing of metasomatic fluids in sigmoid-shaped volumes of fractured host marble. After skarn formation, a mafic magma was emplaced, forming dikelets and filling residual pockets in the skarn. Field evidence and geochemical data show that the "hot" mafic magma interacted with the previously formed Zn-Pb(-Ag) skarn, triggering textural reworking and chemical redistribution of Zn-Pb sulfides as well as contributing to a late an Fe-Cu mineralization. Campiglia Marittima skarn-ore system behaved at odd: a telescoping process is recorded, yet in a reverse way.

1. Introduction

Skarn is a calc-silicate rock resulting from the metasomatism of rocks – usually carbonate-rich ones – by infiltration of hydrothermal fluids (Meinert et al., 2005). Most skarns have an intimate spatial relationship with magmatic intrusions (proximal skarn), although in some cases magmatic hydrothermal fluids may migrate over considerable distances to produce skarn and ore bodies with no clear spatial link to magmatic intrusions (distal skarn; Einaudi et al., 1981; Meinert et al., 2005). Skarn ores, mantos and chimneys (Carbonate Replacement Deposits CRDs; Megaw et al., 1988) and porphyry-type ore deposits are the world's major sources of Cu, Pb, Zn, Ag, and Au (Baker et al., 2004). All these deposits are possibly genetically linked (Einaudi et al., 1981; Titley, 1993).

Good understanding of three-dimensional skarn geometries, ore types and ore forming-processes is important for a correct petrogenetic interpretation. Factors, such as depth of emplacement, composition and location of the magmatic intrusion and nature of the host rocks may lead to the development of either an ore deposit or a barren skarn (Meinert et al., 2005). Among these factors, the distance between the skarn and the causative igneous body is considered extremely important (Meinert et al., 2005; Nakano 1998). For example, most Fe-Cu skarns form in close proximity to magmatic rocks, typically at higher temperatures with respect to distal Zn-Pb skarns (see Meinert et al., 2005 for a review).

Campiglia Marittima (hereafter Campiglia) is an important case study for skarn deposit, in particular, for two reasons: (i) it has been exploited for base metals (Cu, Pb, Zn) and Ag for over twenty-seven centuries, from Etruscan times (7th century BC) to 1979, when mining activity in the area definitely ceased, and (ii) it is considered as a classic example of an exoskarn (Dill, 2010) and a reference model for the development of a contact exoskarn from the causative magmatic rock to the marble host rock (Burt, 1977; Corsini et al., 1980).

The importance of the Campiglia skarn was first noted by Vom Rath (1868), who described it as the first example of internal mineralogical zoning in a metasomatic body. This skarn deposit was later used to model mineralogical zoning in skarns (Bartholomé and Evrard, 1970; Corsini et al., 1980), also by applying the chemical potential approach (Burt, 1977, based on Korzhinskii, 1968). These models are all based on a chronological sequence involving early emplacement of a mafic porphyry dike followed by development of an exoskarn with an outward sequence of three mineral zones: magnetite through ilvaite to clinopyroxene from the mafic dike towards the marble. There are two contrasting explanations for the origin of this zoning: (i) simultaneous development of the three mineralogical zones, with the inner zones continuously replacing the outer ones (Burt, 1977), and (ii) sequential, outward formation of the three zones in a multistage process (Bartholomé and Evrard, 1970; Corsini et al., 1980; Capitani and Mellini, 2000). The skarn development also resulted in ore deposition, producing a sulfide zoning, with Fe-Cu ore in the internal, ilvaite zone and Zn-Pb ore in the external, clinopyroxene zone (Bodechtel, 1968; Corsini and Tanelli, 1974; Capitani and Mellini, 2000). This magmatic-hydrothermal sequence of events corresponds to the "normal sequence" outlined for a number of other skarn deposits (for a review see Meinert et al., 2005).

This classic model has been recently questioned by a new large dataset on the Campiglia skarn including field (20 km^2) and underground (>20 km of tunnels) mapping, as well as petrographic, mineralogical and geochemical data from drill logs (19 km) (Vezzoni et al., 2013; Vezzoni, 2014). These data show that: (i) mafic magma was emplaced after skarn formation in a chronological sequence that is inverse to the one described by existing models; (ii) the three-dimensional geometry of the skarn and magmatic bodies is different from that previously reported; (iii) the fluid pathways controlling skarn formation are planar, multiple and not related to the axial zone of the skarn, as inferred in previous models (Bartholomé and Evrard, 1970; Corsini et al., 1980; Samim, 1983). Based on these findings, we have reconstructed the relative timing and mechanism of skarn and ore formation: the ores formed through two main events, with overprinting of a higher-T sulfide assemblage on a lower-T one, in a sequence that is reversed with respect to a normal telescoping process (Sillitoe, 1994; Heinrich, 2005). The conceptual model developed for Campiglia may find application in other skarn ore systems.

2. Geological setting

The Campiglia area is characterized by a N-S trending horst of Mesozoic carbonate rocks (Tuscan units) surrounded by Jurassic-Eocene ophiolitic-flysch sequence (Ligurian Units). The horst, bounded by high-angle extensional and strike-slip faults, developed as a consequence of extensional tectonics in the inner part of the Apennine thrust-and-fold belt (Fig. 1; Acocella et al., 2000; Rossetti et al., 2000). Extension that began in the Miocene, produced a thinned crust (here ~22 km), widespread magmatism involving both crustal anatectic and mantle-derived products, and diffuse hydrothermal activity that still continues nowadays (Barberi et al., 1967; Dini et al., 2005; Bertini et al., 2006).

The Campiglia carbonate horst was intruded in the late Miocene by a monzogranite pluton (5.7 Ma; Borsi et al., 1967) cropping out at Botro ai Marmi. Mafic and felsic porphyritic dikes crosscut the contact aureole of the monzogranite intrusion (Fig. 1), and an early Pliocene rhyolitic extrusive complex (4.38±0.04 Ma; Feldstein et al., 1994) covers the Ligurian Units and the early Pliocene sediments to the west of the carbonate horst (Barberi et al., 1967).

Skarn and ore concentrations, in close spatial association with the intrusive rocks, occur as: (i) minor metasomatic bodies at the pluton-to-carbonate formation contact (Fig. 1; Barberi et al., 1967); (ii) low-grade veins and disseminations Sn-W-As-Bi ore (Sn~0.4 wt%; Fig. 1; Venerandi-Pirri and Zuffardi, 1982); and (iii) the main Campiglia Fe-Cu-Zn-Pb(-Ag) skarn deposit (Figs. 1 and 2). The Campiglia skarn deposit consists of several bodies and veins that crop out discontinuously between Monte Spinosa to the south and Monte Coronato to the north (Fig. 2). Some of these skarn bodies surround small intrusions of mafic porphyry. Skarn bodies and mafic porphyries are later crosscut by felsic dikes (Figs. 1 and 2; Bodechtel, 1968).

3. Magmatic units

3.1. Botro ai Marmi granite

Magmatism at Campiglia began with the emplacement of the Botro ai Marmi monzogranite pluton (K-feldspar K-Ar date of 5.7 Ma; Borsi et al., 1967). The pluton roof is elongated in a N-S direction, as indicated by data from exploratory wells (Stella, 1955; Grassi et al., 1990), by geophysical data (Aquater, 1994) and by the NE-SW to N-S trending antiformal structure of the foliation in the large contact-metamorphic aureole (Acocella et al., 2000). The aureole consists essentially of marble (developed over a Rhaetian grey platform carbonate) overlain by Hettangian white reef limestones and Sinemurian red nodular limestones (Fig. 1; Acocella et al., 2000; Rossetti et al., 2000).

The primary paragenesis of the monzogranite consists of quartz, K-feldspar, plagioclase and biotite, along with accessory titanite, apatite, zircon and tourmaline. Due to pervasive hydrothermal alteration resulting in increase of K_2O (up to 10 wt%) and loss of Ca, Fe, and S, this assemblage is rarely preserved in the monzogranite (Rodolico, 1945; Barberi et al., 1967), making it unsuitable for quarrying as a raw material for ceramics. The chemical composition is characterized by the occurrence of replacement K-feldspar (as well as primary K-feldspar) and by the disappearance of biotite. Lattanzi et al. (2001) ascribed these features to late- to post- magmatic K-metasomatism.

3.2. Mafic Temperino porphyry

The mafic porphyry unit is found only in the Temperino mining area, where it is spatially associated with skarn bodies. This porphyritic rock is commonly found within skarn bodies and, rarely, at the skarn-marble contact (but never directly intruding the marble). No higher concentration is noted along the axial zone of the skarn bodies. Mafic porphyry occurs as isolated subvertical dikelets (0.3-2 m thick and up to 30 m long) crosscutting the primary skarn textures or as irregular masses with lenticular, spherical, cigar-like shapes and varying in size from several dm^3 to several m^3 (Fig. 3), as seen in all levels of the Temperino mine. The shapes of these irregular porphyry masses match those of the surrounding skarn spheroids (Figs. 3C and D). Closer observation of the boundaries between skarn and porphyry masses reveals that the cm-scale rugged contacts are due to euhedral ilvaite crystals lining the original outer skarn surface (Fig. 3D). The mafic magma was therefore emplaced after skarn formation as dikelets or as infill of primary skarn pockets lined with euhedral crystals of ilvaite (Fig. 3; Vezzoni, 2014).

The mafic Temperino porphyry is a deeply altered porphyritic igneous rock originally containing phenocrysts of plagioclase, biotite, clinopyroxene, orthopyroxene and olivine, along with abundant coarse-grained sanidine and quartz xenocrysts, all set in a fine-grained groundmass. Mafic phenocrysts are transformed into actinolite, epidote, Mg-rich chlorites and carbonates, with only biotite and rare clinopyroxene relicts. The groundmass is completely recrystallized into a fine-grained aggregate of K-feldspar, quartz and chlorite. Accessory minerals are chromite, apatite, zircon, monazite, and ilmenite.

3.3. Coquand and Ortaccio felsic porphyry dikes

The Coquand porphyry is formed by two dikes <10 m thick. The main dike crops out discontinuously for >2 km in a SE-NW direction and connects the Earle, Collins, San Silvestro and Manienti skarn bodies, but crosscuts both the skarn and the mafic Temperino porphyry. The smaller dike cuts the southern part of the Le Marchand body (Fig. 2).

The Ortaccio felsic porphyry dike crops out almost continuously for about 8 km, reaching a maximum thickness >20 meters. This dike crosscuts the other magmatic and metasomatic rocks (Temperino-Lanzi skarn, Temperino mafic porphyry, and Coquand felsic dikes; Fig. 2; Bodechtel, 1968; Vezzoni, 2014). The emplacement age is poorly constrained (whole rock K-Ar date of 4.30±0.13 Ma; Borsi et al., 1967).

The two different types of felsic porphyritic dikes have similar mineralogical characteristics. They carry phenocrysts of quartz, cm-sized sanidine, plagioclase, biotite and pinitized cordierite set in a completely recrystallized, fine-grained groundmass of K-feldspar, quartz and minor “chlorite”. There are mafic enclaves up to 10 cm in size (Fig. 2; Vezzoni, 2014).

3.4. San Vincenzo rhyolite

The San Vincenzo rhyolite represents the closing igneous episode in the Campiglia area (sanidine ^{40}Ar-^{39}Ar date of 4.38±0.04 Ma; Feldstein et al., 1994). The rhyolite was emplaced as a viscous lava flow or dome above the Mesozoic Ligurian Units and the Pliocene sediments, covering a surface area of about 10 km^2 NW of the Campiglia horst.

The rhyolite, which contains rare small mafic enclaves, is a porphyritic rock with phenocrysts of quartz, alkali feldspar, plagioclase and biotite, along with lesser amounts of cordierite. The groundmass consists of plagioclase, biotite and glass, with accessory apatite, monazite, zircon, ilmenite and epidote (Ferrara et al., 1989; Ridolfi et al., 2015).

4. Methods

The present work is based on field observations integrated with petrographic, mineralogical and geochemical data. The research strategy aimed to collect data in order to define: (i) the external geometry of the skarn and the shape of porphyry bodies; (ii) the internal skarn structures and mineralogical zoning; (iii) the textural features, mineralogy and chemistry of skarn silicates and ore minerals.

The new survey carried out on both surface outcrops and in all the accessible underground workings allowed a detailed characterization (geometry, attitude) and sampling (for petrographic, mineralogical and chemical analysis) of the magmatic and metasomatic units (Fig. 2). The underground workings at the Temperino mine consist of two main shafts (named Earle and Le Marchand) connecting six levels within the Earle body, and five levels within the Le Marchand body (ranging in elevation from 290 down to 46 m a.s.l.). At the Lanzi mine, the Walter Shaft connects ten levels (from 380 down to 138 m a.s.l.). Exploitation of the sulfide ores produced large, steeply dipping stopes (up to 140 m high and 900 m^2 in horizontal section) that are still accessible at the Temperino mine but have mostly collapsed at the Lanzi mine.

The abandoned underground workings (adits, shafts, inclined shafts and stopes) at the Temperino and Lanzi mines were mapped in detail thanks to the use of speleological techniques and safety protocols. The walls and roofs of 20 km of tunnels were mapped for a total area in excess of 100,000 m^2 allowing a 3D reconstruction (axonometric projections) of this unique magmatic-metasomatic system (Figs. 3, 4, and 5). Underground mapping was integrated with surface geological survey over an area of 20 km^2. Direct field observations were integrated with data from mining reports and lithological/geochemical logs of 175 diamond and RC drill holes (~19,000 m, performed by SAMIM S.p.A. for the last mining exploration program at Campiglia in the 1980's; Samim, 1983).

The 3D representation, integrated with the geological maps of the underground mining levels and several geological sections, allowed investigation of the internal structure of skarn, mineralogical zoning and ore shoot morphology, and provided insight into spatial relationships with magmatic rocks (as reported in Fig. 6 for Level 3, Earle Shaft).

Polished sections were investigated by means of high-resolution image analysis/scanned images, trasmitted/reflected light optical microscopy, and scanning electron microscopy (SEM, a Philips XL 30 operating at 20 kV), coupled with energy-dispersive X-ray fluorescence spectrometry at the Dipartimento di Scienze della Terra, University of Pisa. During the last mining exploration program, SAMIM S.p.A. completed the geochemical analysis of drill cores via ICP-AES after aqua regia sulfide digestion (Samim, 1983).

5. The skarns: geometry, zoning pattern and internal structures

Campiglia skarn deposits crop out over an area of about 12 km^2 and are commonly hosted in pure marble (Fig. 2). The most common occurrences are represented by Zn-Pb(-Ag) skarns, exploited by the Lanzi mine and its N-S trending, subsidiary array of minor Zn-Pb(-Ag) deposits (Buche al Ferro, Vallin Lungo, Biserno, Manienti, San Silvestro, Aione, Collins and Montorsi). Two peculiar Cu-Fe-Zn-Pb(-Ag) skarn bodies crop out (Earle and Le Marchand) representing the largest ore bodies in the area which were exploited by the Temperino mine. Skarn bodies consist of clinopyroxene and ilvaite, variably developed to produce monomineralic masses of massive ilvaite and/or fibrous-radiating hedenbergite, as well as rhythmically layered hedenbergite-ilvaite aggregates. Andradite is a widespread accessory phase while johannsenite and Mn-pyroxenoids are found as a few small masses (Capitani and Mellini, 2000; Dini et al., 2013). Ore mineral assemblages are dominated by sphalerite, galena, chalcopyrite, pyrrhotite, pyrite and magnetite. Primary pockets of up to several m^3 are a common feature of Campiglia skarns and were dug in the past for the production of exquisite collection specimens with large crystals of ilvaite and quartz (Dini et al., 2013).

5.1. Skarns and igneous units: geometry and spatial relationships

Quantitative analysis of the geometry and spatial relationships between skarn and igneous units is essential in reconstructing the complex magmatic-metasomatic processes that occurred at Campiglia. Previous scientific contributions report detailed petrographic, mineralogical and geochemical-isotopic data on the Temperino deposit, but lack a detailed geological characterization of the skarn bodies. The published maps and cross sections (e.g., Bartholomé and Evrard, 1970; Corsini et al., 1980) actually represent interpretative sketches based on old mining reports, which were strongly influenced by the early scientific hypotheses on Campiglia skarns (e.g., Rodolico, 1931).

Field observations mainly focused on the four major skarn bodies at the Temperino (Earle and Le Marchand) and Lanzi (Lanzi 1 and Lanzi 2) mines. A quick survey was also conducted on all the minor bodies belonging to the N-S trending Zn-Pb(-Ag) skarn array. Three types of skarn occurrences were detected according to their morphology: (i) sigmoids, (ii) tongues, and (iii) veins. Sigmoids are mostly found as large, steeply dipping generally to the NE bodies, crosscutting the subhorizontal marble foliation. Their maximum thickness is 20-40 m, whereas their horizontal and vertical extensions reach 500 and 200 m, respectively. Tongues are gently dipping mantos locally protruding from sigmoids, and are paraconformal with the marble foliation. These tongues branch off the eastern side of the sigmoids, dip variably to the NE, and taper out at depth. Although they were intersected by several tunnels and drill holes, their attitude was never clearly determined (e.g., mining reports; Corsini et al., 1980). Skarn veins are vertical, often with a thickness of a few mm to some tens of cm. They form parallel arrays starting from the hangingwalls and footwalls of both sigmoids and tongues and taper out with distance. Below the main sigmoids (root zone), the deepest drillholes (e.g., drill hole C1; Fig. 3) intersected larger skarn veins, some of which were intruded by the mafic porphyry.

The largest skarn is the Earle body; based on 3D mapping and reconstruction, its total volume is of the order of $1.6x10^6$ m^3. It consists of a large subvertical body with a gently NE-dipping lateral tongue (Fig. 3A). The Earle body has a sigmoid-tabular shape akin to a mega-tension gash, reaching its maximum thickness in the central portion (>40 m; Level 3 Earle Shaft), and tapering out southwestward at the upper termination and northeastward at the lower termination (consisting of two separate limbs). The mafic Temperino porphyry occurs most commonly as subvertical dikelets with rounded to pointy tips. The mafic porphyry also occurs as masses with highly variable attitude, size (1 to >10 m^3) and shape (lenticular, spherical, cigar-like, irregular). These porphyry masses represent the negative shapes of preexisting primary pockets in the skarn (Figs. 3C and D). As a whole, the mafic Temperino porphyry represents ~10 vol% of the Earle skarn body, although the porphyry/skarn volume ratio, as well as the average size of porphyry masses, increases with depth. The Coquand porphyry felsic dike cuts across the central portion of the subvertical Earle body, which has the same strike (150N) and dip. The Ortaccio porphyry felsic dike crosscuts at high angle both the skarn and the Coquand dike (Fig. 3B).

The total volume of the Le Marchand skarn body is estimated at some $1.4x10^6$ m^3. Similarly to the Earle body, the Le Marchand skarn is a subvertical sigmoid-tabular body (Fig. 4) with two minor gently dipping tongues branching off to the NE (Fig. 4C). Relationships between magmatic rocks and skarn are similar to those described for the Earle body. The mafic Temperino porphyry represents 5 vol%, with the porphyry/skarn volume ratio and the average size of porphyry masses increasing with depth. As for the Earle skarn, the Coquand porphyry felsic dike intrudes concordantly the SE part of the Le Marchand body and is crosscut by the Ortaccio porphyry dike.

The Lanzi mine exploited two skarn bodies with a total volume of $0.2x10^6$ m^3 and no association with magmatic rocks. The main Lanzi body is made of a partly coalescing cluster of small sigmoid-tabular bodies that make up a tabular body striking 040N and dipping steeply (70-80°) to the SE (Fig. 5). The northeastern side of the main Lanzi skarn body is characterized by several small subhorizontal tongues. At the Lanzi mine, numerous well-developed skarn veins branch off the skarn mass, tapering out within a few tens of meters. The host marble shows a well-developed and closely spaced (few cm) array of subvertical, parallel fractures with preferential 025N strike. Fractures and skarn veins have the same attitude, but only fractures intersecting skarn bodies contain skarn veins (Fig. 5C). The minor Lanzi skarn body consists of several subhorizontal bodies with decimetric to metric thickness that strikes around N030, 30NW and are connected by subvertical veins (Fig. 5).

5.2. Mineral zoning pattern and primary pockets in the skarn

The Campiglia skarn bodies are characterized by three different skarn facies in which the main phases, ilvaite and hedenbergite, have variable relative abundances and textures: (i) rhythmically layered hedenbergite-ilvaite (Fig. 7A); (ii) fibrous-radiating hedenbergite (Fig. 7B); (iii) massive ilvaite (Fig. 7C). Only the fibrous-radiating hedenbergite facies occurs at the Lanzi mine, whereas the three facies are well represented at the Temperino mine, with most of the skarn volume made of rhythmically layered hedenbergite-ilvaite and massive ilvaite facies (Da Mommio et al., 2010; Figs. 3B and 6). Minor skarn bodies in the area also display all the three facies.

The rhythmically layered facies is made of alternating, nearly monomineralic layers (1 mm - 20 cm) of hedenbergite and ilvaite. Most of the layers have an overall near-planar geometry generated by the coalescence of contiguous spheroidal sectors. Layering thus consists of multiple planar-convex layers with an overall NW-SE subvertical attitude. Locally, especially around primary pockets, some spheroidal sectors become dominant, producing prominent large banded spheroids (up to 1 m in radius) responsible for the typical shape of the pockets (Fig. 7B). Around large pockets (also up to 10 m^3) or clusters of pockets, a common sequence of multiple planar-convex layers and banded spheroids can be observed all around the cavities. These show significant lateral continuity with constant thicknesses: in mine tunnels a single ilvaite or hedenbergite band can be followed for tens of meters.

The fibrous-radiating hedenbergite facies consists of spheroidal aggregates of fibrous hedenbergite crystals, with the longest fibers reaching up to 50 cm in length; randomly distributed spheroids are common. The residual space between coalescing spheroids often forms pockets with typical scalloped shape (e.g., Figs. 3C and 7B) and size generally not exceeding 1 m^3. Locally, e.g. at the San Silvestro skarn body, the Mn content in pyroxene is high enough to generate a johannsenite fibrous-radiating facies associated with pyroxmangite and rhodonite (Capitani and Mellini, 2000).

The massive ilvaite facies is formed by an extremely cohesive granular aggregate of ilvaite crystals ranging from 0.1 to 5 mm in size. Ilvaite is generally not preferentially oriented, although parallel layers with comb texture do occur. Residual pockets in this facies are quite rare and are typically <1-3 dm^3 in size.

Skarn bodies at the Lanzi mine consist of hedenbergite only, whereas ilvaite is found almost exclusively as euhedral crystals lining primary pockets. At the Temperino mine, the three facies are irregularly arranged, in contrast to the classic model of symmetrical zoning. Even the classic Coquand Section shows no symmetrical zoning (Da Mommio et al., 2010). In Level 3 of the Earle body, there is again no systematic zoning but a reverse mineral zoning, with the occurrence of massive ilvaite at the skarn-marble contact (Fig. 3B).

The primary paragenesis of the skarn bodies is sometimes partially or completely replaced by secondary smectite-montmorillonite and Fe-oxi-hydroxides (Fig. 7D). Such pervasive oxydation/hydration mostly occurs in minor skarn bodies and along late N-S-trending vertical fractures. The original fibrous-radiating clinopyroxene texture is sometimes partially preserved, whereas ilvaite is mainly replaced by massive and earthy Fe-hydroxides. Sulfides were pervasively oxidized, allowing the formation of a large number of Pb-Zn-Cu carbonates, sulphate-carbonates and hydrous silicates (e.g., smithsonite, hemimorphite, cerussite, auricalcite, brochantite, serpierite, campigliaite; Conticini et al., 1980; Biagioni et al., 2013). These altered volumes, called “morbidone” (i.e. very soft material) by miners, were preferentially exploited by ancient Etruscan and medieval miners.

A prominent feature of the Campiglia skarns is the large number of primary cavities (up to several m^3 in size) occurring in the internal portions of the skarn bodies (Dini et al., 2013). These pockets lead to a significant primary macroporosity of the skarn, with implications on deposition of sulfide ores and emplacement of mafic magma after the formation of the metasomatic bodies (see next sections). The pocket shape is highly variable, from irregular, roughly spheroidal, tubular to oblate. The pockets represent 2-15% of the skarn volume and are not homogeneously distributed, frequently clustering along vertical planes in the internal zones of the skarn bodies. The pockets are lined by idiomorphic crystals of ilvaite (up to 8 cm long) and/or hedenbergite, grown as the latest phases of the skarn system. Some of the pockets are later filled with mafic porphyry. Later on, low-temperature quartz (Belkin et al., 1983; Agrosi et al., 1992) partially/totally filled both most of the remaining empty pockets and rare residual voids in porphyry-filled pockets.

5.3. Directional growth textures

The Campiglia skarns are characterized by directional textures such as diverging fibrous-radiating clinopyroxene aggregates and multiple planar-convex layers (Figs. 3C and 6A) of both ilvaite and hedenbergite. Directional textures allow reconstructing the pattern of crystallization during skarn formation. These textures indicate the direction and sense of mineral growth (growth versors) based on the following assumptions, coming also from some igneous examples (e.g., Lofgren, 1971): (i) the mineral growth direction is parallel to the elongation of hedenbergite and orthogonal to the mineral layering; (ii) the growth sense is indicated by the fanning out of the hedenbergite fibers and the convexity of the multiple planar-convex layers (Abrecht, 1985; Rusinov & Zhukov, 2008).

The most suitable area in which this textural analysis has been applied is mining Level 3 of the Earle skarn body (Temperino mine; Fig. 5). The skarn body there has been explored, and partially exploited, by a main tunnel and several closely spaced crosscuts connecting vertical stopes. Different skarn facies, mafic and felsic dikes, as well as ore-filled and large empty pockets are well exposed. Measurements were mainly performed on vertical surfaces perpendicular to the strike of the skarn body. Most of the data were collected in rhythmically layered hedenbergite-ilvaite facies and in small volumes of fibrous-radiating hedenbergite facies. The massive texture of the ilvaite facies hampered the definition of any sense of growth.

The resulting growth versors map (Fig. 6A) shows that growth directions strike mostly SW-NE (Fig. 6B) with a subhorizontal dip (Fig. 6C), i.e. orthogonal to the margins of the skarn. In particular, the growth versors do not indicate a common direction but are grouped in NW-SE-oriented zones that are parallel to the attitude of the skarn body. Within each zone, growth versors systematically show coherent strikes, with senses defining an inward convergence pattern from the external boundaries towards a linear axial core zone also marked by the occurrence of large primary pockets (some empty, some filled with mafic porphyry) and high-grade orebodies. At least three main coherent growth zones have been observed, with inward sense of growth as indicated by their growth patterns, in contrast to the single symmetric outward model proposed previously (e.g., Corsini et al., 1980). The direction and sense of growth deviates from the overall trend just around the primary pockets in skarn, which mostly occur at the core of growth zones. Here, the mineral growth versors are centripetal around the cavities (Fig. 6D).

A similar growth pattern has been mapped in all other levels of the Earle skarn, even if the discontinuous outcrops make it difficult to determine growth zones throughout the skarn body. Nevertheless, some growth zones and their axial pockets can be followed from the surface outcrops down to Level 4, some 120 m below the surface. Note that mafic porphyry dikelets and the later felsic porphyry dikes (Coquand and Ortaccio) intersect the skarn growth zones, cutting across skarn textures such as mineral fibers and layers/spheroids (Figs. 3B and 6).

6. Mineralizations: types, geometry, mineralogy and geochemistry

The overall production of base metals at Campiglia during the second half of the 20th century (when most of the ore was extracted) was 0.15 Mt, corresponding to a very small portion of the large volume of the clinopyroxene-ilvaite skarn (~$3x10^6$ m^3). These values resulted from the occurrence of large volumes of barren/low-grade skarn hosting small sparse medium- to high-grade ore shoots. The main ore shoots are invariably hosted within the internal portions of the skarn bodies, whereas the skarn-marble contacts are only rarely mineralized. The Lanzi and Temperino mines exploited three different types of ore: (i) Zn-Pb(-Ag) type; (ii) Cu-Fe type; (iii) Zn-Pb-Cu(-Ag) type. The Zn-Pb(-Ag) ore type is never associated with magmatic rocks (e.g., Lanzi mine), whereas the Cu-Fe ore type is intimately associated with the masses of mafic porphyry that intruded the skarn bodies. The Zn-Pb-Cu(-Ag) ore type occurs systematically in association with Cu-Fe ore and mafic porphyry bodies (only at the Temperino mine).

6.1. *The Zn-Pb(-Ag) ore type*

The Zn-Pb(-Ag) ore type is found throughout the N-S-trending belt extending from Montorsi to Buche al Ferro (Fig. 2), including the main Zn-Pb(-Ag) skarn of the Lanzi mine. At the Temperino mine, small masses of this ore type occur in areas where intrusions of mafic porphyry are lacking. The Zn-Pb(-Ag) ore type is characterized by fine- to medium-grained aggregates (mostly < 5 mm) of sphalerite and galena, along with very minor pyrite. Tetrahedrite has been rarely observed in late quartz veinlets. Sulfides post-date the formation of the calc-silicate skarn, occurring as fracture infill, disrupted primary cavities and brecciated portions of the metasomatic bodies. The most common textures include: (i) clast- and matrix-supported breccias cemented by Zn-Pb sulfides passing to massive sulfide bodies containing scattered clasts of clinopyroxene/ilvaite skarns (Fig. 8A); in a few cases, clinopyroxene was partially or totally hydrated to amphibole; (ii) cm-thick veins crosscutting the skarn

(Fig. 9A); (iii) mm- to cm-thick sulfide layers that propagate from veins into scallop-shaped cracks between growth layers of fibrous-radiating clinopyroxene (Fig. 9B).

Zn-Pb sulfides are not homogeneously distributed, and most of the production at Lanzi came from two high-grade ore shoots (average Zn+Pb = 6.2 wt%; Pb/Zn = 0.56) (from mining reports; Samim, 1983) embedded in barren and/or very low-grade skarn. Fe-poor sphalerite (1-3 wt% Fe; Corsini and Tanelli, 1974) is more abundant than galena, although a progressive increase in galena and Ag content (from ~800 to 1800 ppm Ag in galena) was observed in the lowermost portions of the ore shoots (Bodechtel, 1968). These ores were almost completely exploited before 1960. Ore shoots displayed a flat pipe geometry with the main axis subparallel to the dip of the sigmoid bodies and the intermediate axis parallel to the strike of the skarn body. The main skarn body at Lanzi hosted an ore shoot which was almost continuous (Fig. 10A) from the surface outcrops (330 m) down to Level 6 (218 m). The ore shoot in the minor skarn body has a similar geometry, but is significantly smaller and tapers out at a shallower depth (Level 4; 260 m). Considering the calculated volumes of the skarn bodies (~200,000 m^3, from mapping) and of the ore shoots (~85,000 m^3, from mining reports), the mineralized portion represented about 40% of the total volume of the metasomatic bodies. Mapping of the accessible underground stopes revealed a lower (~30%) percentage, which is still higher than at the Temperino mine (~14%, see below). Continuous ore shoots have been observed only at the Lanzi mine; other Zn-Pb(-Ag) skarn deposits in the area (Buche al Ferro, Vallin Lungo, Biserno, Manienti, San Silvestro, Aione and Collins) host smaller, irregular sulfide bodies.

6.2. The Cu-Fe ore type

The Cu-Fe ore occurs only at the Temperino mine, where it represents the dominant ore in the Earle skarn body, whereas in the Le Marchand skarn body it is associated with significant volumes of the Zn-Pb-Cu(-Ag) ore type (next section). The Cu-Fe ore invariably overprints the skarn at the contact with the mafic porphyry masses and dikelets, producing variable replacement and infill textures (Figs. 7C, 8B, and C). The mineral assemblage is dominated by chalcopyrite, pyrrhotite and pyrite, along with minor magnetite. The intrusion of mafic porphyry into the skarn produced a narrow band (up to 10 cm thick) of cryptocrystalline magnetite and hedenbergite after ilvaite (Fig. 8B), which is commonly overprinted by a larger band (up to 30 cm) of high-grade, massive chalcopyrite-pyrrhotite-pyrite containing up to 10 wt% Cu and devoided of Zn and Pb (Fig. 9C). Partial to total replacement and pervasive veining of both skarn and magnetite reaction bands occurred in this narrow shell surrounding the mafic porphyry bodies. Low- to medium- grade Cu-Fe ore (up to 3-4 wt% Cu) consisting of chalcopyrite, pyrrhotite, pyrite and magnetite extends in the nearby skarn volumes for several meters/tens of meters. Mineralization occurs as veins (Fig. 7C), partial filling of primary pockets, interstitial disseminations and irregular replacement bodies (fine- to coarse-grained disseminated and massive ore). Ilvaite – both massive bodies and euhedral crystals from primary pockets – was selectively replaced by iron sulfides and chalcopyrite (Figs. 8B, C, and 9C), whereas hedenbergite was replaced by the same sulfide assemblage sometimes in association with actinolite, chlorite and garnet (Fig. 9D). Andradite and fluorite represent common late phases associated with actinolite, pyrite, chalcopyrite, and axinite-(Mn) in veins and interstitial patches of quartz in the Cu-Fe ore (Dini et al., 2013).

Iron-rich sphalerite (9-12 wt% Fe; Corsini and Tanelli, 1974; Gregorio et al., 1977) locally occurs as an interstitial late phase and as star-like inclusions in chalcopyrite within low-grade Cu-Fe ores (up to 0.6 wt% Zn). Bismuth sulfides are common in Cu-Fe ore, both in low- and high- grade zones. Emplectite ($CuBiS_2$) was reported by Bodechtel (1968), whereas galenobismutite ($PbBi_2S_4$, Lopez-Ruiz et al., 1969) occurs as prismatic crystals included in early magnetite and in late quartz and fluorite veinlets. Bismuthinite (Bernardini et al., 1974) is found as prismatic crystals in chalcopyrite, and Ag-rich cosalite ($Pb_2Bi_2S_5$; Ag = 0.4-1.3 wt%) occurs in late quartz and fluorite veinlets (Fig. 8D).

The shapes of the multiple Cu-Fe ore shoots exploited at the Temperino mine are less regular than those of the Zn-Pb(-Ag) Lanzi ore shoots (Figs. 10B and C). The Cu-Fe ore is spatially related to the mafic porphyry bodies, the locations and shapes of which are controlled by the original primary porosity of skarn (clusters/trails of large pockets), which is mainly limited to the internal portions of the skarn bodies. The largest high-grade ore shoots were exploited in the upper portions of the skarn bodies, although the relative amount of mafic porphyry tends to increase at depth. In only two cases the mafic magma dikes are emplaced at the skarn-marble contact, producing a decimetric band of Cu-Fe sulfides at the contact with marble. The average Cu grade for the Cu-Fe ore type (from mining reports and drilling data; Samim, 1983) was in the range of 1.9-2.7 wt%, with negligible Pb and locally poor zinc contents (< 0.6 wt%).

Three main southeast-dipping ore shoots were exploited within the sigmoid Earle skarn body (Fig. 10C): two ore shoots (E1 and E2) were dug since Etruscan time from outcrops (~220-260 m a.s.l.) down to Level 3 (114 m) and Level 4 (82 m); a third ore shoot (E3) discovered at depth was exploited from Level 1 (178 m) down to Level 6 (45 m). Note that the high-grade Cu-Fe ore tends to be confined to the upper part of the skarn body, with ore shoots tapering out northwards at progressively lower elevations. These are associated with minor volumes of Zn-Pb-Cu(-Ag) ore occurring in the upper part of the sigmoid body (from Level 1 to the surface) and in tongue C1 branching off from the eastern upper contact. The Le Marchand skarn body hosted three northeast-dipping Cu-Fe ore shoots: two large ore bodies (LM1 and LM2) were exploited from the surface (280-260 m a.s.l.) down to Level 5 (115 m), a third ore shoot was intersected at Level 1 (212 m) and excavated down to Level 4 (153 m). The LM2 ore shoot has a quite continuous flat pipe morphology (Fig. 10B), whereas the two other ore shoots show a more irregular geometry. These Cu-Fe ore shoots are associated with large irregular masses of Zn-Pb-Cu(-Ag) ore (see next chapter).

The new data from underground mapping, coupled with that from old mining reports, indicates that ore shoots at the Temperino mine occupied 11-17 % of the total volume of the skarn bodies (Earle body: 1.6×10^6 m^3; Le Marchand body: 1.4×10^6 m^3). This estimate matches the results obtained during the last drilling exploration campaign (~19,000 m of diamond or RC holes; Samim, 1983), which indicate that 14% of the borehole-skarn intersections are mineralized. For the Earle body this estimate is indicative of the Cu-Fe ore only, whereas for the Le Marchand body the estimate includes both Cu-Fe and Zn-Pb-Cu(-Ag) ores in equal proportions.

6.3. The Zn-Pb-Cu(-Ag) ore type

The Zn-Pb-Cu(-Ag) ore occurs mainly in the Le Marchand skarn body (Temperino mine), where it is intimately associated with the Cu-Fe ore and invariably overprints the skarn, forming scattered irregular bodies locally interfingered with low- to medium-grade Cu-Fe ore but not in contact with any of the mafic porphyry masses/dikelets. The mineral assemblage is dominated by sphalerite and galena with minor chalcopyrite, pyrite and rare magnetite (see also Corsini et al., 1980, and references therein). Most of the ore bodies are characterized by a coarse-grained dendritic and wedge-shaped elongated crystals of galena (up to 5 cm) intergrown with sphalerite in granular and fan-shaped aggregates of feathery crystals (up to 6 cm). Significant amounts of chalcopyrite are found in some hand specimens, although at the outcrop scale this mineral is a minor constituent forming low-grade Cu ore (<1 %). Chalcopyrite forms anhedral aggregates that fill interstices and fractures within the Zn-Pb sulfides (Figs. 9E and F), and in some cases it forms intergrowths, mostly with galena. Sphalerite is extremely and heterogeneously zoned (1 to 12 wt% Fe; Corsini and Tanelli, 1974) and, when associated with chalcopyrite veins/patches, it is characterized by a micrometer- to submicrometer-sized chalcopyrite dusting/veining. The same texture also occurs in sphalerite in contact with galena (in association with chalcopyrite; Figs. 11B, C, and D) and quartz veins containing isolated grains of garnet, and chalcopyrite (Figs. 9D, 11E, and F). Chalcopyrite disseminations and veinlets are randomly distributed, and their abundance quickly decreases within the first few micrometers/millimeters of the contact with chalcopyrite masses and quartz veins. Most chalcopyrite grains occur along the sphalerite grain boundaries, as revealed by etching (Bernardini et al., 1974).

Ore shoots are discontinuous, and underground observations, coupled with drill core data, suggest that they have an irregular lenticular shape. Zn-Pb-Cu(-Ag) ore shoots differ from the previous two ore types by commonly spreading out from the internal portions of the skarn bodies towards the contacts with marble. Ore bodies are locally rich in sulfides (massive sulfide zones; up to 50 wt% Zn+Pb+Cu), yet the average ore grades are significantly lower (Zn+Pb = 8.6 wt%; Pb/Zn = 0.58; Cu = 0.5 wt%) (from mining reports and drilling data; Samim, 1983). Direct observations in all accessible underground stopes, coupled with calculation from production data, indicate that the Zn-Pb-Cu(-Ag) ore type represents about half of the extracted ore from the Le Marchand body (ore shoot volume equal to 11-17 % of the total skarn volume; see previous section).

6.4. Mineral chemistry of the ore deposit

During the 20th century, mining companies focused their activity on the Lanzi and Temperino skarn bodies, where mining operations continued until 1959 and 1979, respectively. Internal mining reports on sulfide ores extracted during the periods 1950-59 (Lanzi mine) and 1970-75 (Temperino mine) have been used to estimate the average relative proportion of Cu, Pb, and Zn. The average Pb/Zn ratio is 0.56±0.12 SD for Lanzi and 0.64±0.18 SD for Temperino, two similar values typical of distal Zn-Pb skarn deposits (Samson et al., 2008; Williams-Jones et al., 2010).

Numerous drill core logs, coupled with chemical analyses, were carried out in the 1980s to investigate the grade and morphology of ore bodies at depth (Samim, 1983) and to identify the nature of the two main magnetic anomalies recorded in the Temperino mine area (Fig. 2; Aquater, 1994). This dataset is used in the present study to compare the textural and mineralogical characteristics of the Temperino and Lanzi ore bodies. Chemical data for the Temperino mineralizations were considered analytically representative when Pb+Zn ≥ 0.5 wt%, or when Cu ≥ 0.3 wt%. After this screening, 246 data points were plotted on a binary Pb/(Pb+Zn+Cu) vs. Zn/(Pb+Zn+Cu) diagram (Fig. 12A). In this plot, the main ore types are distributed as follows. The Zn-Pb(-Ag) ore has a Pb/Zn ratio of between 0.4 and 0.8 and is poor in Cu. The Cu-Fe ore contains little Zn (<0.6 wt%) and negligible Pb. The Zn-Pb-Cu(-Ag) ore has a highly variable Pb/Zn ratio and a variable Cu content (up to 3 wt%). Note that the overall observed compositional variability at the scale of the whole ore deposit (Fig. 12A) is replicated at the scale of single ore shoots, e.g. in the Le Marchand Level 4-5 body (Figs. 12B, C, and D).

7. Discussion

The Cu-Zn-Pb(-Ag) skarn deposits at Campiglia represent an excellent opportunity to investigate relationships between magmatic rocks, skarn and sulfide ores. Our new field observations integrated with petrographic and mineralogical data provide insight into the spatial-temporal evolution of a multi-stage hydrothermal system related to the sequential emplacement of different magma batches in the shallow crust.

7.1. The classical Campiglia exoskarn model revisited

Campiglia skarn deposits were considered as a classic example of exoskarn developed due to the emplacement of a magma (mafic porphyry) that triggered the progressive replacement of marbles by skarn and the subsequent deposition of sulfides (e.g., Rodolico 1931; Bartholomé and Evrard, 1970; Corsini et al., 1980). The skarn has been described as having an outward symmetric mineralogical zoning with respect to a hypothetical axial mafic porphyry dike. A zoning sequence has been proposed for both the main skarn minerals (porphyry ⇒ magnetite ⇒ ilvaite ⇒ clinopyroxene ⇒ marble) and the ore minerals (chalcopyrite + pyrrhotite in magnetite/ilvaite zones ⇒ sphalerite + galena in hedenbergite zone) (Bartholomé and Evrard, 1970; Corsini & Tanelli, 1974). This evolution is in agreement with the classic model of Korzhinskii (1968), and theoretically consistent with the evolutionary paths proposed by Burt (1977) on the basis of chemical potential diagrams. This model was mainly developed for the Earle body at the Temperino mine, making the Campiglia skarns a reference example for exoskarn formation processes (Dill, 2010).

This work presents a revised chronological sequence of events. The mafic magma was emplaced after skarn formation, given that it formed dikelets and filled large primary pockets in the skarn bodies (Fig. 3; Vezzoni et al., 2013; Vezzoni, 2014). Mafic magma invaded the skarn bodies at Temperino mine, crosscutting both hedenbergite and/or ilvaite and controlling the distribution of Cu-Fe orebodies. The outward mineralogical zoning of the skarn is also reconsidered taking into account the direct contact between the massive ilvaite facies and the marble host rock, as well as the widespread occurrence of rhythmically layered ilvaite-hedenbergite skarn facies (e.g., Fig. 3B). The Temperino skarn bodies are not mineralogically zoned, and the more external zones are formed by either ilvaite or hedenbergite, as visible in the Coquand Section (Da Mommio et al., 2010) and in Level 3 of the Earle body. Some authors (Burt, 1977) have also suggested that the symmetrical skarn zones developed simultaneously as a result of chemical potential gradients existing between iron- and silica- rich solutions and marble host rocks, with the innermost zones continuously replacing the outer ones. This hypothesis, although attractive from a chemical perspective, is not supported by field and petrographic data: at the Temperino mine, large volumes of rhythmically layered ilvaite-hedenbergite skarn indicate that the physico-chemical conditions did oscillate tens of times between ilvaite and hedenbergite stability, respectively, with no evidence for reciprocal replacement.

Furthermore, a primary magnetite skarn zone has not been observed; instead, a magnetite + hedenbergite assemblage developed after ilvaite at the contact with the mafic porphyry (Vezzoni, 2014). This is coherent with a heating process triggered by the mafic magma, in accordance with experimental studies on ilvaite (Gustafson, 1974) showing that the reaction:

$$12 \text{ ilvaite} + O_2 \rightarrow 12 \text{ hedenbergite} + 8 \text{ magnetite} + 6\ H_2O$$

develops at T > 470 °C in a wide range of $f(O_2)$. The reaction stoichiometry indicates production of 69.5 vol% hedenbergite and 30.5 vol% magnetite, in close agreement with the mineral proportions observed in the reaction band. Magnetite reaction bands, as well as disseminated magnetite in the Cu-Fe sulfide ore, overprint the primary skarn silicates and their spatial distribution matches that of the mafic porphyry in the skarn bodies.

Further evidence of the lack of symmetrical, outward skarn growth from a single axial magmatic dike (Burt, 1977; Corsini et al., 1980) is seen in the skarn mineral growth versors map (e.g., Level 3 of the Earle body; Fig. 6): the crystals grew outwards from multiple planes parallel to the skarn edges. The convergence areas amid these planes are characterized by centripetal growth versors in which spheroids and planar-convex layers merge, sometimes leaving central primary pockets. Around primary pockets, growth versors deviate from the average subhorizontal NE-SW attitude, showing all possible orientations, even vertical at the floor/roof of the pockets. The rhythmically layered hedenbergite-ilvaite facies highlight these features, as the monomineralic skarn bands form continuous layers (planar-convex layers) with persistent thickness that can be traced along strike for tens of meters. Lateral continuity and thickness are also maintained around pockets of both small and large size (up to several tens of m^3), suggesting rather homogeneous mineral growth in each layer, despite the large area and the variation in orientation (around pockets) of the crystallization surfaces. This crystallization geometry mimics textures observed in epithermal chalcedony-quartz veins (crustiform/comb/banded textures with vugs; e.g., Dong et al., 2005) and in agate geodes (Wang and Merino, 1990; Taijing and

Sunagawa, 1994), which are ascribed to crystallization in an open space. The occurrence of open spaces when the fluid arrived would require a mechanism more complex than simple replacive metasomatism: these open volumes must be ascribed to a process other than fluid-rock interaction. Structural-mineralogical data can help assess the possible role of local tectonics in this context.

7.2. Emplacement mechanisms for fluids and magmas

The reconstructed three-dimensional geometries, mineralogical zoning and mineral growth versors of Campiglia skarns are important in reconstructing the permeability paths and traps exploited by hydrothermal fluids and magmas. The homogeneous, massive nature of the marble host rock allowed the free development of structures under the direct control of external stress only, without the influence of pre-existing lithological anisotropies or discontinuities. The geometry of skarn bodies can thus be a key to understanding deformational processes operating during the magmatic-hydrothermal event.

The Tuscan Magmatic Province is characterized by the emplacement of tabular intrusions - plutons, laccoliths, and sills - at very shallow crustal levels (to depths of 2-5 km; Dini et al., 2002; Rocchi et al., 2010) under dominant extensional conditions. Magma accumulation at shallow crustal levels enhanced movements along low-angle detachment faults, inducing ductile deformation in contact aureoles and brittle deformation outside the aureole and in the upper plate (e.g., Elba Island; Westerman et al., 2004; Caggianelli et al., 2014). In particular, the lateral displacement of the overburden accelerated the exhumation of the intrusions at the surface, producing a switch from lithostatic to hydrostatic conditions in the associated hydrothermal systems (Maineri et al., 2003).

In the Campiglia area such a scenario would provide a working model for interpreting the geometries of the skarn bodies. These bodies have an overall steeply-dipping, sigmoid shape and are interpreted as large-scale tension gash-type structures. Their position and geometry is compatible with the activity of a low-angle extensional fault zone with a top-to-the-east sense of movement at the contact between the carbonatic and the overlying mainly pelitic/arenitic formations. The sigmoidal skarn bodies did not simply form by filling dilational jogs – as in true tension gashes – but are the product of fluid metasomatism of a sigmoid-shaped volume of fractured marble. This damaged marble volume thus acted as a relatively low-pressure zone that drew metasomatic fluids from depth. Successive batches of fluids gathered within this fractured volume led to the dissolution of marble, followed by the centripetal growth of the skarn minerals. This interpretation reconciles the field evidence with the current skarn formation model in which decarbonation reactions enhance permeability in the host-rock (Ortoleva et al., 1987; Yardley and Lloyd, 1995; Meinert et al., 2005). However, the nature of the skarn-forming fluids at Campiglia and elsewhere is still a matter of investigation. The available data from other skarn systems are indeed restricted to microthermometry approaches and chemical data on skarn-forming fluids are rare (e.g., Baker et al., 2004; Samson et al., 2008; Willliams-Jones et al., 2010).

Repetitive, synchronous mineralogical layers developed in such a scenario, sometimes leaving empty pockets of variable size (Figs. 3C, D, 4B, 6D, 7A, and 8B). The absence of marble relicts and the widespread presence of primary pockets at the center of each growth zone supports this model.

The minor, gently NE-dipping skarn tongues on the eastern sides of the main sigmoidal skarn bodies developed on a minor marble foliation, drawing fluids from the main evolving skarn volumes in the top-to-the-east extensional setting.

The close spatial and/or geometric relationships between skarn and magmatic rocks suggest similar emplacement mechanisms during the same tectonic regime. The Temperino mafic porphyry is found only within the skarn, where it formed dikelets and the infill of large primary pockets. The felsic Coquand porphyry dike mainly intruded the skarn bodies; it mostly follows their sub-vertical sigmoidal shape. The orientation of the Ortaccio felsic late porphyry dike has no link to the skarn, attesting to a final change in the local stress regime.

A unique local tectonic-magmatic extensional stress regime was thus responsible for the fracturing of the marble, the ascent and circulation of early skarn-forming fluids, as well as for the final ascent and emplacement of mafic and felsic (Coquand) dikes. This type of kinematics, based on the activity of top-to-the-east extensional zones enhanced (steepened) by pluton emplacement, played an important role in determining the distribution (in the lower plate), geometry (sigmoidal bodies) and paragenetic sequence (Cu-Fe overprinting on Zn-Pb ores) of Campiglia skarns.

7.3. Reverse telescoping and sulfide remobilization at Campiglia

Overprinting of early, usually deep-seated mineralizations (e.g., porphyry type and Cu and Fe- skarn) by late, shallower, generally epithermal precious- and base-metal mineralizations is described as telescoping (Sillitoe, 1994). This process is generally attributed to the lowering of the paleosurface due to rapid erosion or to the sector collapse of an overlying stratovolcano with the extensive ingress of meteoric water in the magmatic environment and a decrease in confining pressure (e.g., Sillitoe, 1994; Sillitoe and Hedenquist, 2003; Redmond et al., 2004; Heinrich et al., 2004; Heinrich, 2005).

This common worldwide scenario contrasts with that of the Campiglia skarn-ore system, for which a reverse telescoping process is recorded. The emplacement of mafic magma in the distal Zn-Pb skarns, was both activating prograde back-reactions (ilvaite to magnetite + hedenbergite) and Mg-rich overgrowths on early hedenbergite fibers (Vezzoni, 2014), and triggering the overprinting of high-temperature Fe-Cu sulfide ore onto the lower-temperature Zn-Pb sulfide assemblage. The addition of Fe-Cu, as well as the local remobilization of earlier Zn-Pb ores, led to the formation of the mixed Zn-Pb-Cu(-Ag) ore, as documented by field observations, skarn-ore textural observations, drill core chemical data and bulk ore-grade ratios.

Several lines of evidence support the reverse telescoping interpretation. First, most of the skarn bodies at Campiglia, including the Lanzi mine and portions of skarn bodies at the Temperino mine, host Zn-Pb(-Ag) ores only and are not directly associated with magmatic rocks. Skarn mineralogies and textures are all characterized by ore shoots with a flat pipe morphology and consisting of fine-grained aggregates of galena and yellow-green to orange-brown Fe-poor sphalerite. They display the typical chemical characteristics of distal Zn-Pb skarn deposits, including a slightly variable composition with Pb/Zn ratios ranging between 0.4 and 0.8 (0.56 average) and negligible amounts of copper (Fig. 12). The Pb/Zn ratio is in the compositional range of ores (~ 0.1 to 2 with an average grade of 0.29) and fluid inclusions (0.1 to 1.7 with a median value of 0.63) from similar skarn deposits (e.g., El Mochito, Honduras; Samson et al., 2008; Williams-Jones et al., 2010). This homogeneity vanishes abruptly at the site of the two pronounced magnetic anomalies in the Temperino mine (Fig. 2), where the skarn was invaded by the mafic magma and partly replaced by magnetite. Here, the Cu-Fe ore shoots display a close causative relationship with the mafic porphyry intrusions, overprinting both skarn minerals and Pb-Zn(-Ag) ores. Cu-Fe ores are dominated by copper (up to 10 wt%; average 1.9-2.7 wt%) with only a small amount of zinc (< 0.6 wt%; mainly in iron-rich interstitial sphalerite) and negligible lead.

Overprinting of Cu-Fe ore onto Zn-Pb(-Ag) ores is indicated by field, textural and geochemical data. Cu-Fe ore shoots in the Le Marchand body are significantly continuous from the surface down to the deepest levels, and are surrounded by very irregular masses of galena and sphalerite associated with significant amounts of chalcopyrite: the Zn-Pb-Cu(-Ag) ore type. The coarse-grained, dendritic and feathery texture, the extremely heterogeneous galena/sphalerite modal ratio, the extensive skarn replacement up to the marble contacts and the chalcopyrite veining and co-precipitation with galena are all macroscopic characteristics suggesting the reworking of pre-existing Zn-Pb(-Ag) ores by Cu-Fe-rich fluids. At the micro scale there is also a clear relationship between Cu-Fe-rich fluids and sphalerite recrystallization, as suggested by the chalcopyrite dusting and veining in sphalerite (Figs. 11B, C, D, E, and F), and by the extremely variable sphalerite composition (from 1 to 12 wt% Fe; Corsini and Tanelli, 1974; Gregorio et al., 1977).

If the conversion of Zn-Pb(-Ag) ore to Zn-Pb-Cu(-Ag) ore had been a simple recrystallization with the addition of Cu, the metal ratios of the new ore assemblage would have plotted on straight lines connecting the Cu-Fe ores and the Zn-Pb(-Ag) ores, e.g., the theoretical mixing line in Figure 13. Instead, the Zn-Pb-Cu(-Ag) ore data show a completely different pattern: with respect to the pristine Zn-Pb(-Ag) ore, the new assemblage experienced strong chemical reworking and compositional spreading so that it covers the entire range from the Zn to the Pb end-members. Chemical reworking occurred randomly at every scale, from cm to tens of m, precluding the development of a “zone refining” process and a laterally zoned ore body (as proposed for the Volcanic Massive Sulfide Kuroko deposits; Ohmoto, 1996). Some copper and iron were added to the original chemical components, which were just spatially re-arranged. For this reason, a single ore body/outcrop/drill core intersection from the Temperino mine can provide the whole spectrum of compositions (Figs. 12B, C, and D) reported in the total diagram (Figs. 12A and 13). Copper addition did not occur through simple mixing between two end-members, but through a mixing "front" that shifted the products of the ongoing remobilization (the Zn-Pb-Cu(-Ag) ore) towards the Cu-Fe ore corner. The significant compositional gap between Cu-Fe ore and Zn-Pb-Cu(-Ag) ore in Figure 13 indicates that mafic magma intruded the skarn mainly along the available primary porosity (empty pockets). Most of the Cu-Fe-rich fluids deposited ore in the nearby barren skarn and eventually interacted with the previously formed Zn-Pb(-Ag) orebodies.

The reverse telescoping process, triggered by the intrusion of mafic magma, locally (Temperino mine) added an "exotic" component (Cu) to the distal Zn-Pb(-Ag) skarn complex of Campiglia, producing the unusual overprinting of a typical proximal high-T sulfide assemblage over a distal lower-T one (Fig. 14). A similar scenario has been described for the giant (100 Mt) Zn-Pb(-Ag) Kamioka skarn deposits in Japan (Mariko et al., 1996). In this case there is no evidence of a direct intrusion of magmas in the mineralized skarn, and the Cu-Fe ores have been ascribed to the influx of fluids that interacted with different magmatic and metamorphic rocks. Late crystallization of chalcopyrite in distal Zn-Pb(-Ag) skarns has been described in other mining areas such as Madan (Bulgaria; Bonev, 1977) and in the Nikolaevsky Mine (Russia; Rogulina and Sveshnikova, 2008). Reverse telescoping may thus have been an active process in other districts where late fluids impacted the skarn leaving the magma behind, whereas in Campiglia the causative magma intruded the telescoped skarn.

In normal telescoping, lowering of the paleosurface is directly responsible for the overprinting of high-T ore systems by low-T epithermal mineralization. In the Campiglia case, the removal of overburden by extensional low-angle faulting (related to magma accumulation in the shallow crust, as in other Tuscany magmatic complex (Elba Island: Westerman et al., 2004; Dini et al., 2008) triggered the ascent and emplacement of mafic magma, thus transferring from a deep to a shallow setting the heat source responsible for the reverse telescoping process.

8. Conclusions

The Campiglia area represents an excellent case study for investigating different types of skarn-related mineralizations closely linked to multiple magmatic events. The rough zoning of ore types in the Temperino mining area could at first seem related to the "normal" temporal and spatial evolution of a hydrothermal system: the highest temperature Fe-Cu paragenesis appears to be located close to a mafic intrusion, whereas the outer Zn-Pb paragenesis could be related to the waning stage of the hydrothermal system. On the contrary, this work reveals that the Zn-Pb skarn predates the Fe-Cu mineralization and formed as a distal skarn having no spatial relationship with magmatic rocks, as would be expected in this type of skarn deposit (e.g., Einaudi et al., 1981; Meinert et al., 2005).

This work thus proposes a new relative timing and reconstruction of magmatic-hydrothermal events in the area (Fig. 14). In an extensional tectonic regime, the metasomatic fluids rose up to form primary skarn silicate minerals and Zn-Pb(-Ag) ore (Fig. 14A). A batch of mafic magma was then emplaced, causing both textural reworking of the Zn-Pb sulfide ore and chemical reworking with addition of Fe-Cu (Fig. 14B). The two ore mineralizations are typical of two different environments: Fe-Cu ore is characterized by the highest formation temperatures and is proximal to the mafic intrusion, whereas Zn-Pb(-Ag) ore developed in the distal part of the hydrothermal system characterized by lower temperatures (Meinert et al., 2005). Based on these geological characteristics we suggest that the Temperino ore deposit is an example of reverse telescoping in which a typical high-temperature, proximal paragenesis overprints an earlier, distal-type ore mineralization. In this model, the emplacement of mafic magma is not required, given that deep hydrothermal fluids can be emplaced independently. Nevertheless, in the Temperino mining area the magma did intrude the skarn deposits, allowing the straightforward interpretation of odd paragenetic sequences. The three hypothetical drill logs depicted in Figure 14B show how apparently different types of ore-body zoning can be observed when a mafic magmatic body is present but does not crop out. The reverse telescoping process can thus explain the uncharacteristic zoning and evolution of the skarn deposit, i.e. the prograde, then retrograde stages.

In light of these findings, it might be worth reassessing examples where late Cu-bearing paragenesis are seen to overprint previously formed Zn-Pb ores: the evidence for reverse telescoping in distal systems could be a marker for the proximity of higher-T deposits hidden at depth.

In summary, Campiglia skarn deposits can no longer be considered a classic example of proximal exoskarn deposits. They are instead an important example of distal Zn-Pb(-Ag) skarns that experienced a reverse telescoping process. Detailed underground geological mapping and reprocessing of drilling/mining data has led to a significant revision of existing models. Furthermore, knowledge of the geometry and internal structure of bodies has opened new scenarios in which skarns provide information on both fluids and the magmatic-tectonic evolution of the shallow continental crust. In conclusion, detailed 3D mapping of skarn deposits still represents an essential part of any state-of-the-art analytical contribution on this topic.

Acknowledgements

Research was supported by the “Ministero dell’Istruzione, dell’Università e della Ricerca” of Italy (PRIN project: 2008PN8Z9K). Thanks are due to Parco Archeominerario di San Silvestro (Parchi Val di Cornia S.p.A.) for granting access and sampling in the Temperino and Lanzi mining area and to Marco Pistolesi and Luca Tinagli for helping during field surveys. Thoughtful comments by three anonymous reviewers contributed to the improvement of the original manuscript.

REFERENCES

Abrecht, J. (1985). Manganesiferous pyroxenes and pyroxenoids from three Pb-Zn-Cu skarn deposits: Contributions to Mineralogy and Petrology, v. 89, p. 379-393.

Acocella, V., Rossetti, F., Faccenna, C., Funiciello, R. and Lazzarotto, A. (2000). Strike-slip faulting and pluton emplacement in Southern Tuscany: the Campiglia case: Bollettino Società Geologica Italiana, v. 119, 10, p. 517-528.

Agrosi, G., Lattanzi, P., Ruggieri, G., and Scandale, E. (1992). Growth history of a quartz crystal from growth marks and fluid inclusions data: Neues Jb. Miner. Monat., v. 7, p. 289-294.

Aquater (1994). Area Campigliese, Convenzione Ministero Industria, Commercio e Artigianato - ENI: Relazione conclusiva sui lavori svolti. Internal report, 111 p.

Baker, T., Van Achterberg, E., Ryan, C. G. and Lang, J. R. (2004). Composition and evolution of ore fluids in a magmatic-hydrothermal skarn deposit: Geology, v. 32, 2, p. 117-120.

Barberi, F., Innocenti, F. and Mazzuoli, R. (1967). Contributo alla conoscenza chimico-petrografica e magmatologica delle rocce intrusive, vulcaniche e filoniane del Campigliese (Toscana): Memorie Società Geologica Italiana, v. 6, 643-681.

Bartholomé, P. and Evrard, P. (1970). On the Genesis of the Zoned Skarn Complex at Temperino, Tuscany: International Union of Geological Science, Serie A, v. 2, 53-57.

Belkin, H. E., De Vivo, B., and Lattanzi , P. (1983). Fluid inclusion studies on ore deposits of Tuscan Maremma, Italy: Memorie Società Geologica Italiana, v. 25, p. 273-284.

Benvenuti, M., Boni, M. and Meinert, L. D. (2004). Skarn deposits in Southern Tuscany and Elba Island (Central Italy): Field Trip Guide Book - B18, 24 p.

Bernardini, G. P., Corsini, F. and Tanelli, G. (1975). Galena and chalcopyrite from the skarn-sulphide deposit (Valle del Temperino), Campiglia, Tuscany: Rendiconti della Società Italiana di Mineralogia e Petrologia, v. 30, 2, p. 585-595.

Bertini, G., Casini, M., Gianelli, G. and Pandeli, E. (2006). Geological structure of a long-living geothermal system, Larderello, Italy: Terra Nova, v. 18, 3, p. 163-169.

Biagioni, C., Orlandi, P., Cerri, M., Pistolesi, M., Rapaccini, S. and Santucci, A. (2013). Temperino e Lanzi. Le paragenesi secondarie dello skarn: Rivista Mineralogica Italiana Campiese. Miniere e minerali, v. 1, p. 40-55.

Bodechtel, J. (1968). Die Paragenesen der Skarnlagerstatten in den Monte di Campiglia-Toskana. Freiberg: Forschungshefie, 231, 7-20.

Bonev, I. K. (1977). Primary fluid inclusions in galena crystals. I. Morphology and origin: Mineralium Deposita, v. 12, 1, p. 64-76.

Borsi, S., Ferrara, G. and Tongiorgi, E. (1967). Determinazione con il metodo K/Ar delle età delle rocce magmatiche della Toscana: Bollettino Società Geologica Italiana, v. 86, p. 403-411.

Burt, D. M. (1977). Mineralogy and petrology of skarn deposits: Rendiconti della Società Italiana di Mineralogia e Petrologia, v. 33, 2, p. 859-873.

Burt, D. M. (1982). Skarn deposits; historical bibliography through 1970: Economic Geology, v. 77, 4, p. 755-763.

Caggianelli, A., Ranalli, G., Lavecchia, A., Liotta, D. and Dini, A. (2014). Post-emplacement thermo-rheological history of a granite intrusion and surrounding rocks: the Monte Capanne pluton, Elba Island, Italy: Geological Society, London, Special Publications, v. 394, 1, p. 129-143.

Capitani, G. C. and Mellini, M. (2000). The crystallisation sequence of the Campiglia skarn: Neues Jahrbuch für Mineralogie Monatshefte, v. 3, p. 97-115.

Conticini, F., Menchetti, S., Sabelli, C. and Trosti-Ferroni, R. (1980). Minerali di alterazione dei giacimenti a solfuri misti di Campiglia Marittima (Toscana): Rendiconti della Società Italiana di Mineralogia e Petrologia, v. 36, 1, p. 295-308.

Corsini, F. and Tanelli, G. (1974). Analisi alla microsonda elettronica delle blende del giacimento della Valle del Temperino (Campiglio, Toscana): Rendiconti della Società Italiana di Mineralogia e Petrologia, v. 30, 1, p. 205-221.

Corsini, F., Cortecci, G., Leone, G. and Tanelli, G. (1980). Sulfur isotope study of the skarn-(Cu-Pb-Zn) sulfide deposit of Valle del Temperino, Campiglia Marittima, Tuscany, Italy: Economic Geology, v. 75, 1, p. 83-96.

Da Mommio, A., Iaccarino, S., Vezzoni, S., Dini, A., Rocchi, S., Brocchini, D., Guideri, S. and Sbrilli, L. (2010). Valorizzazione del geosito <<Sezione Coquand>>, Miniera del Temperino (Parco Archeominerario di San Silvestro Campiglia): Atti Società Toscana di Scienze Naturali, Memorie, Serie A, v. 115, p. 55-72.

Dill, H. G. (2010). The "chessboard" classification scheme of mineral deposits: Mineralogy and geology from aluminum to zirconium: Earth-Science Reviews, v. 100, 1-4, p. 1-420.

Dini, A., Innocenti, F., Rocchi, S., Tonarini, S. and Westerman, D. S. (2002). The magmatic evolution of the late Miocene laccolith-pluton-dyke granitic complex of Elba Island, Italy: Geological Magazine, v. 139, 3, p. 257-279.

Dini, A., Gianelli, G., Puxeddu, M. and Ruggieri, G. (2005). Origin and evolution of Pliocene–Pleistocene granites from the Larderello geothermal field (Tuscan Magmatic Province, Italy): Lithos, v. 81, p. 1-31.

Dini, A., Mazzarini, F., Musumeci, G. and Rocchi, S. (2008). Multiple hydro-fracturing by boron-rich fluids in the Late Miocene contact aureole of eastern Elba Island (Tuscany, Italy): Terra Nova, v. 20, 4, p. 318-326.

Dini, A., Orlandi, P. and Vezzoni, S. (2013). Temperino e Lanzi. Le paragenesi primarie dello skarn: Rivista Mineralogica Italiana Campigliese. Miniere e minerali, v. 1, p. 28-39.

Dong, G., Morrison, G. and Jaireth, S. (1995). Quartz textures in epithermal veins, Queensland; classification, origin and implication: Economic Geology, v. 90, 6, p. 1841-1856.

Einaudi, M. T., Meinert, L. D. and Newberry, J. (1981). Skarn Deposits: Economic Geology, 75th Anniversary Volume, p. 317-391.

Feldstein, S. N., Halliday, A. N., Davies, G. R. and Hall, C. M. (1994). Isotope and chemical microsampling: Constraints on the history of an S-type rhyolite, San Vincenzo, Tuscany, Italy: Geochimica et Cosmochimica Acta, v. 58, 2, p. 943-958.

Ferrara, G., Petrini, R., Serri, G. and Tonarini, S. (1989). Petrology and isotope-geochemistry of San Vincenzo rhyolites (Tuscany, Italy): Bulletin Volcanologique, v. 51, p. 379-388.

Grassi, S., Squarci, P., Celati, R., Calore, C., Perusini, P. and Taffi, L. (1990). Nuove conoscenze sul sistema idrotermale di Campiglia Marittima (Livorno): Bollettino della Societa Geologica Italiana, v. 109, 4, p. 693-706.

Gregorio, F., Lattanzi , P. and Tanelli, G. (1977). A contribution to the genetic knowledge of the skarn-sulfides deposit of Valle del Temperino (Campiglia Marittima, Toscana): sphalerite, pyrite and pyrrhotite assemblage: Rendiconti Società Italiana di Mineralogia e Petrologia, v. 33, 1, p. 125-134.

Gustafson, W. I. (1974). The Stability of Andradite, Hedenbergite, and Related Minerals in the System Ca-Fe-Si-O-H: Journal of Petrology, v. 15, 3, p. 455-496.

Heinrich, C. (2005). The physical and chemical evolution of low-salinity magmatic fluids at the porphyry to epithermal transition: a thermodynamic study: Mineralium Deposita, v. 39, 8, p. 864-889.

Heinrich, C. A., Günther, D., Audétat, A., Ulrich, T. and Frischknecht, R. (1999). Metal fractionation between magmatic brine and vapor, determined by microanalysis of fluid inclusions: Geology, v. 27, 8, p. 755-758.

Heinrich, C. A., Driesner, T., Stefánsson, A. and Seward, T. M. (2004). Magmatic vapor contraction and the transport of gold from the porphyry environment to epithermal ore deposits: Geology, v. 32, 9, p. 761-764.

Korzhinskii, D. S. (1968). The theory of metasomatic zoning: Mineralium Deposita, v. 3, 3, p. 222-231.

Lattanzi, P., Benvenuti, M., Costagliola, P., Maineri, C., Mascaro, I., Tanelli, G., Dini, A. and Ruggieri, G. (2001). Magmatic versus hydrothermal processes in the formation of raw ceramic material deposits in southern Tuscany: International Symposium on Water-Rock Interaction, 10th, Villasimius, Italy, 10-15 July 2001, p. 725-728.

Lofgren, G. (1971). Spherulitic textures in glassy and crystalline rocks: Journal of Geophysical Research, v. 76, 23, p. 5635-5648.

Lopez-Ruiz, J., Bartholome, P. and Evrard, P. (1969). La galénobismuthine dans le skarns de Campiglia, province de Livourne, Italie: Annales de la Société Géologique de Belgique, v. 92, p. 397-406.

Maineri, C., Benvenuti, M., Costagliola, P., Dini, A., Lattanzi, P., Ruggieri, G. and Villa, I. (2003). Sericitic alteration at the La Crocetta deposit (Elba Island, Italy): interplay between magmatism, tectonics and hydrothermal activity: Mineralium

Deposita, v. 38, 1, p. 67-86.

Mariko, T., Kawada, M., Miura, M. and Ono, S. (1996). Ore Formation Processes of the Mozumi Skarn-type Zn-Pb-Ag Deposit in the Kamioka Mine, Gifu Prefecture, Central Japan - A Mineral Chemistry and Fluid Inclusion Study: Resource Geology, v. 46, 6, p. 337-354.

Megaw, P. K. M., Ruiz, J. and Titley, S. R. (1988). High-temperature, carbonate-hosted Ag-Zn-Pb(Cu) deposits of northern Mexico: Economic Geology, v. 83, 8, p. 1856-1885.

Meinert, L. Dipple, G. M. and Nicolescu, S. (2005). World Skarn Deposits: Economic Geology, 100th Anniversary Volume, p. 299-336.

Nakano, T. (1998). Pyroxene geocheminstry as an indicaor for skarn metallogenesis in Japan, *in* Lentz, D.R., ed., Mineralized intrusion-related skarn systems, Québec City, Canada, Mineralogical Association of Canada, Short Course, v. 26, p. 147-167.

Ohmoto, H. (1996). Formation of volcanogenic massive sulfide deposits: The Kuroko perspective: Ore Geology Reviews, v. 10, p. 135-177.

Ortoleva, P., Chadam, J., Merino, E. and Sen, A. (1987). Geochemical self-organization II: the reactive-infiltration instability: American Journal of Science, v. 287, p. 1008-1040.

Redmond, P. B., Einaudi, M. T., Inan, E. E., Landtwing, M. R. and Heinrich, C. A. (2004). Copper deposition by fluid cooling in intrusion-centered systems: New insights from the Bingham porphyry ore deposit, Utah: Geology, v. 32, 3, p. 217-220.

Rocchi, S., Westerman, D. S., Dini, A. and Farina, F. (2010). Intrusive sheets and sheeted intrusions at Elba Island, Italy: Geosphere, v. 6, 3, p. 225-236.

Rodolico, F. (1931). Ricerche sulle rocce eruttive recenti della Toscana - Le rocce del Campigliese: Atti Società Toscana di Scienze Naturali, Memorie, v. 41, p. 197-251.

Rodolico, F. (1945). Ragguagli sul granito del Campigliese: Atti Società Toscana di Scienze Naturali, v. 52, p. 125-132.

Rogulina, L. I. and Sveshnikova, O. L. (2008). The Nikolaevsky base-metal skarn deposit, Primorye, Russia: Geology of Ore Deposits, v. 50, 1, p. 60-74.

Rossetti, F., Faccenna, C., Acocella, V., Funiciello, R., Jolivet, L. and Salvini, F. (2000). Pluton emplacement in the Northern Tyrrhenian area, Italy: Geological Society of America, Special Papers, v. 174, p. 55-77.

Rusinov, V. and Zhukov, V. (2008). Model for the development of rhythmically banded wollastonite-hedenbergite skarns at the Dal'negorsk deposit, southern Russian Far East: Geochemistry International, v. 46, 8, p. 789-799.

Samim (1983). Nota conclusiva sulle ricerche nella miniera di Campiglia Marittima (Zn - Pb - Cu) - (Toscana). Internal report, 36 p.

Samson, I. M., Williams-Jones, A. E., Ault, K. M., Gagnon, J. E. and Fryer, B. J. (2008). Source of fluids forming distal Zn-Pb-Ag skarns: Evidence from laser ablation-inductively coupled plasma-mass spectrometry analysis of fluid inclusions from El Mochito, Honduras: Geology, v. 36, 12, p. 947-950.

Sillitoe, R. H. (1994). Erosion and collapse of volcanoes: Causes of telescoping in intrusion-centered ore deposits: Geology, v. 22, 10, p. 945-948.

Sillitoe, R. H. and Hedenquist, J. W. (2003). Linkages between Volcanotectonic Settings, Ore-Fluid Compositions, and Epithermal Precious Metal Deposits, *in* Simmons, S.F., Graham, I., eds., Volcanic, Geothermal and Ore-Forming Fluids: Rulers and Witnesses of Processes within the Earth, 1st ed.: Court Boulder, USA, Society of Economic Geologists, Inc., Special Publication, v. 10, p. 315-343.

Stella, A. (1955). La miniera di stagno di Monte Valerio e i giacimenti del Campigliese nel quadro della catena metallifera toscana: Bollettino Società Geologica Italiana, v. 74, p. 109-218.

Taijing, L. and Sunagawa, I. (1994). Texture formation of agate in geode: Mineralogical Journal, v. 17, 2, p. 53-76.

Titley, S. R. (1993). Characteristics of high temperature carbonate-hosted massive sulfide ores in the United States, Mexico and Peru. Mineral deposit modeling, *in* Kirkham, R.V., Sinclair, W.D., Thorpe, R.I., Duke, J.M., eds., Mineral Deposit Modeling: Geological Association of Canada, Special Paper, v. 40, p. 585-614.

Venerandi-Pirri, I. and Zuffardi, P. (1982). The Tin Deposit of Monte Valerio (Tuscany, Italy): Pneumatolytic-Hydrothermal or Sedimentary-Remobilization Processes? Ore Genesis: G. C. Amstutz, G. Frenzel, C. Kluthet al, Springer Berlin Heidelberg, v. 2, p. 57-65.

Vezzoni, S., 2014. Evolution of a pluton-porphyry-skarn system: the Temperino-Lanzi mine (Campiglia Marittima, Tuscany): Unpublished PhD thesis, Pisa, Italy, Università di Pisa, 205 p.

Vezzoni, S., Dini, A., Rocchi, S., 2013. Magma emplacement and sulfide deposition after skarn formation at Campiglia Marittima, Italy: Goldschmidt conference 2013, Florence, Italy, 25 - 30 August 2013, Goldschmidt2013 Conference Abstracts, p. 2412

Vom Rath, G. (1868). Die Berge von Campiglia in der Toskanischen Maremme: Zeitschrift der Deutschen Geologischen Gesellschaft, v. 20, p. 307-364.

Wang, Y. and Merino, E. (1990). Self-organizational origin of agates: Banding, fiber twisting, composition, and dynamic crystallization model: Geochimica et Cosmochimica Acta, v. 54, p. 1627-1638.

Westerman, D. S., Dini, A., Innocenti, F. and Rocchi, S. (2004). Rise and fall of a nested Christmas-tree laccolith complex, Elba Island, Italy: Geological Society, London, Special Publications, v. 234, p. 195-213.

Whitney, D. L. and Evans, B. W. (2010). Abbreviations for names of rock-forming minerals: American Mineralogist, v. 95, p. 185-187.

Wilkinson, J. J., Stoffell, B., Wilkinson, C. C., Jeffries, T. E. and Appold, M. S. (2009). Anomalously Metal-Rich Fluids Form Hydrothermal Ore Deposits: Science, v. 323, p. 764-767.

Williams-Jones, A. E. and Heinrich, C. A. (2005). 100th Anniversary Special Paper: Vapor Transport of Metals and the Formation of Magmatic-Hydrothermal Ore Deposits: Economic Geology, v. 100, 7, p. 1287-1312.

Williams-Jones, A. E., Samson, I. M., Ault, K. M., Gagnon, J. E. and Fryer, B. J. (2010). The Genesis of Distal Zinc Skarns: Evidence from the Mochito Deposit, Honduras: Economic Geology, v. 105, 8, p. 1411-1440.

Yardley, B. W. D. and Lloyd, G. E. (1995). Why metasomatic fronts are really metasomatic sides: Geology, v. 23, 1, p. 53-56.

FIGURE CAPTIONS

Fig. 1. (A) Location map of the Campiglia area (modified from Da Mommio et al., 2010) and (B) schematic geological map.

(1.5 column width, no color in print version)

Fig. 2. Interpretive map of the magmatic and hydrothermal units. Magnetic anomaly values are reported as a difference with respect to the local background (after Aquater, 1994). Scans images of rock slabs from the Campiglia magmatic units on the right.

(1.5 column width, no color in print version)

Fig. 3. (A) 3D-reconstruction of the Earle skarn body (Temperino mine) based on geological survey data and drill logs. (B) Geological map of Level 3 of the Earle body (Temperino mine) showing the distribution of the three different skarn facies. (C) and (D) Metric-sized skarn pockets filled by the mafic Temperino porphyry (Level 3 Earle body, Temperino mine).

(2 column width, no color in print version)

Fig. 4. (A) 3D reconstruction of the Le Marchand skarn body (Temperino mine) based on geological survey data and drill logs. (B) The largest primary skarn pocket filled by mafic Temperino porphyry identified at Campiglia (Level 4 Le Marchand body, Temperino mine); (C) Meter-size subhorizontal tongue of the skarn body (Level 4 Le Marchand body, Temperino mine). Dashed lines indicate the marble foliation.

(1.5 column width, no color in print version)

Fig. 5. (A) 3D reconstruction of the Lanzi mine skarn bodies based on geological survey data. (B) and (C) Relationships between marble fractures and skarn veins (Lanzi mine); (D) Decimetre-sized sigmoid-tabular skarn body, similar to a tension gash, at the bottom of the main skarn body (Interlevel 2-3, Lanzi mine).

(1.5 column width, no color in print version)

Fig. 6. (A) Spatial distribution and orientation of the skarn mineral growth versors (blue arrows), Level 3 of the Earle body, Temperino mine. Blue lines indicate the traces of sub-vertical planes from which mineral growth versors diverge; solid lines: well constrained plane traces; dashed lines: inferred plane traces. (B) Rose diagram of

the strikes of growth versors. C) Histogram of the plunges of growth versors. (D) Close-up of two skarn pockets filled with mafic porphyry; the skarn growth versors are centripetal with respect to the pockets (see also Fig. 6A, B).

(1.5 column width, no color in print version)

Fig. 7. Representative photographs of the different skarn facies. (A) rhythmically layered hedenbergite-ilvaite facies; note the large skarn pocket filled by mafic Temperino porphyry, as well as the skarn mineral growth versors pointing towards it (Earle body, Temperino mine). (B) Fibrous-radiating hedenbergite facies; note the small skarn pocket left after the growth of the spheroidal hedenbergite, which developed in the direction of the arrows. The skarn pocket was later partially filled by euhedral quartz crystals (Earle body, Temperino mine). (C) Massive ilvaite facies cut by Fe-Cu sulfide veins (Earle body, Temperino mine). (D) Partly oxidized hedenbergite skarn in which the original fibrous-radiating texture is preserved (Le Marchand body, Temperino mine).

(1.5 column width, no color in print version)

Fig. 8. (A) Zn-Pb(-Ag) ore from the Lanzi mine. (B) Contact between mafic Temperino porphyry filling a residual pocket and an ilvaite skarn layer, detail of Figs. 3C, and D; ilvaite is partly replaced by hedenbergite + magnetite and Fe-Cu sulfides. (C) Ilvaite replaced by Fe-Cu sulfides in rhythmically layered hedenbergite-ilvaite facies from Le Marchand body, Temperino mine. (D) BSE-SEM image of a quartz vein near a mafic porphyry-filled pocket from Gran Cava adit, Temperino mine, showing the occurrence of late cosalite crystals at the Temperino mine. Abbreviation of mineral names after Whitney and Evans (2010): chalcopyrite (Ccp), galena (Gn), hedenbergite (Hd), ilvaite (Ilv), magnetite (Mag), pyrite (Py), pyrrhotite (Po), quartz (Qz), sphalerite (Sp).

(1.5 column width, no color in print version)

Fig. 9. Scanned images of rock slabs representative of the Campiglia ores. (A) Fine-grained sphalerite + galena in Zn-Pb(-Ag) ore from the Lanzi mine. (B) Cm-thick sphalerite + galena sulfide layer in Zn-Pb(-Ag) ore from the San Silvestro ore body,

Gallerione mine. (C) Chalcopyrite + pyrrhotite, Cu-Fe ore from the Le Marchand body, Temperino mine. (D) Chalcopyrite masses and veinlets with actinolite and andradite in hedenbergite, Cu-Fe ore from the Earle body, Temperino mine. (E) Relationships between sphalerite, galena, and chalcopyrite in a Zn-Pb-Cu-Fe(-Ag) ore body, Le Marchand body, Temperino mine; sulfide crystals are coarse-grained and galena shows dendritic crystals. (F) Sphalerite + galena + chalcopyrite layers between spheroids of hedenbergite, Zn-Pb-Cu-Fe(-Ag) ore from the Le Marchand body, Temperino mine. Abbreviations of mineral names after Whitney and Evans (2010): actinolite (Act), andradite (Adr), calcite (Cal), chalcopyrite (Ccp), galena (Gn), hedenbergite (Hd), ilvaite (Ilv), johannsenite (Jhn), magnetite (Mag), pyrite (Py), pyrrhotite (Po), quartz (Qz), sphalerite (Sp).

(2 column width, no color in print version)

Fig. 10. Geological sections and ore body morphologies. (A) Transversal sections of the Ortaccio ore shoot, Temperino mine and (B) Lanzi body 1 ore shoot. (C) Longitudinal section of the Earle skarn body.

(1.5 column width, no color in print version)

Fig. 11. Reflected light photomicrographs of Campiglia ores. (A) Sphalerite + galena with minor quartz from the Lanzi mine. (B) Galena and chalcopyrite in sphalerite with broken pyrite crystals from the Temperino mine. (C) Close-up of the chalcopyrite grains in sphalerite seen in B. (D) Chalcopyrite grains in sphalerite at the contact between chalcopyrite and sphalerite, from the Temperino mine. (E) Chalcopyrite grains in sphalerite at the contact between galena and sphalerite, from the Temperino mine. (F) Chalcopyrite grains in sphalerite at the contact between andradite and quartz, from the Temperino mine; note the well-defined outer limit of the chalcopyrite grains in sphalerite. Abbreviations of minerals from Whitney and Evans (2010): andradite (Adr), chalcopyrite (Ccp), galena (Gn), pyrite (Py), quartz (Qz), sphalerite (Sp.)

(2 column width, no color in print version)

Fig. 12. Zn/(Pb+Zn+Cu) vs. Pb/(Pb+Zn+Cu) binary diagrams based on chemical

data from drill core samples (after Samim, 1983) with (A) the average value of the three ore bodies (Zn-Pb(-Ag), Fe- Cu, Zn-Pb-Cu(-Ag)). B), C), and D) show the data from a single Zn-Pb-Cu(-Ag) ore body (Level 4-5 Le Marchand body, Temperino mine) with total Cu, Zn, and Pb values for each sample. Values are displayed in grey scale with size of bubbles proportional to metal concentration values.

(1.5 column width, no color in print version)

Fig. 13. Zn/(Pb+Zn+Cu) vs. Pb/(Pb+Zn+Cu) binary diagrams based on chemical data from drill core samples and showing the total production of the Lanzi and Temperino mines. Square symbols indicate data from Zn-Pb(-Ag) ore bodies, circles from Fe-Cu ore bodies, triangles from Zn-Pb-Cu(-Ag) ore bodies. The dotted line indicates the theoretical mixing line for the simple addition of Cu on previously formed Zn-Pb(-Ag) ore with a Pb/Zn ratio of 0.56 (average value from the Lanzi mine production).

(1.5 column width, no color in print version)

Fig. 14. Schematic evolution model of a reverse telescoping system. A) Stage 1 - distal Zn-Pb(-Ag) skarn deposit: primary skarn silicate formation and Zn-Pb(-Ag) ore body deposition (Lanzi mine type). B) Stage 2 - Reverse telescoping Zn-Pb-Cu(-Ag) skarn deposit: emplacement at shallow crustal levels of a mafic magma and Fe-Cu ore deposition on a Zn-Pb(-Ag) distal skarn deposit formed earlier (Temperino mine type). Note: three hypothetical geological core logs through the ore deposit are reported on the right. They could be interpreted as related to "normal" skarn evolution in the absence of field constraints from the relative chronology and structure of skarns, ores and magmatic rocks.

(2 column width, no color in print version)

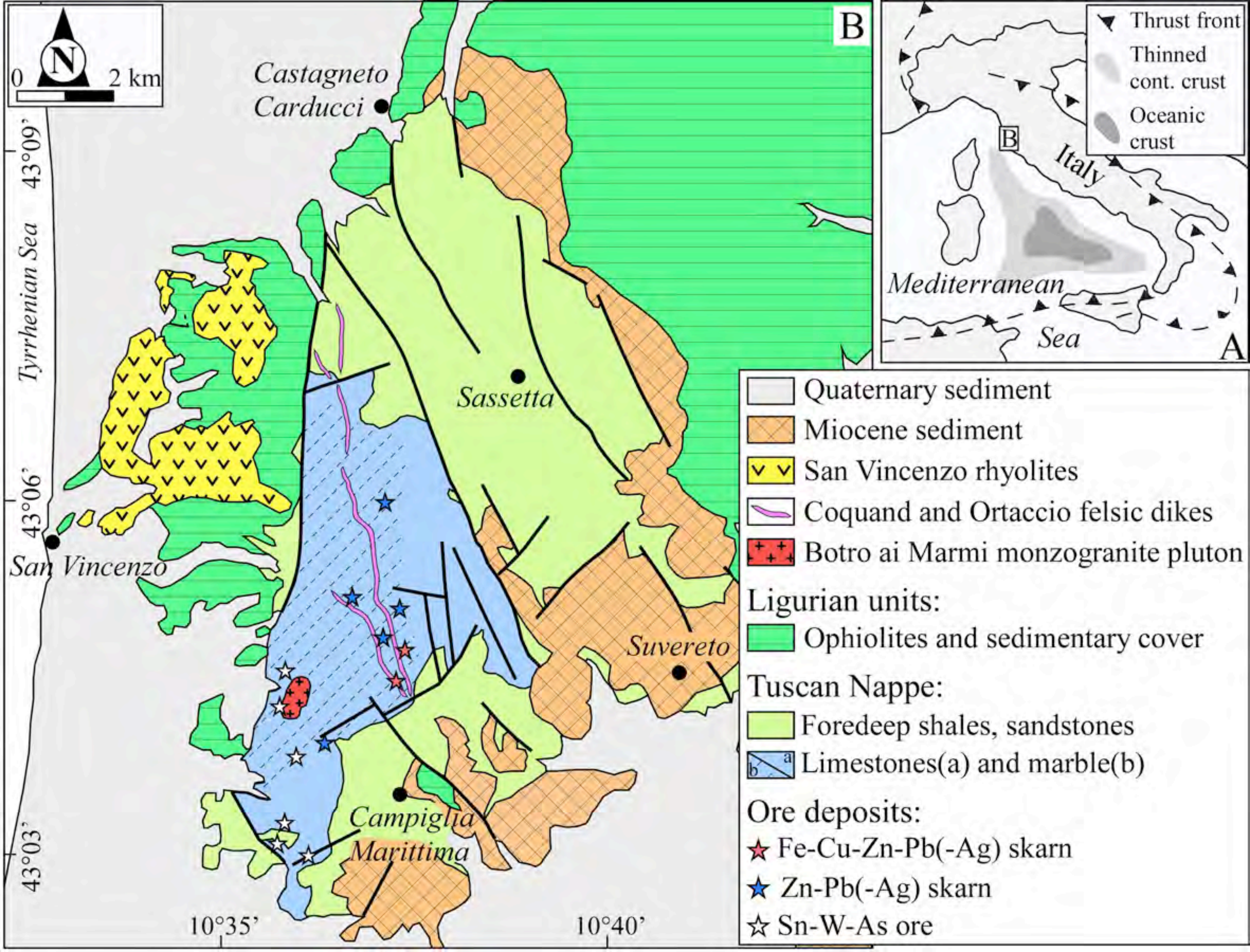
B
0
2 km
N
Castagneto
Carducci
43°09'
Tyrrhenian Sea
43°06'
San Vincenzo
Sassetta
Suvereto
Campiglia
Marittima
43°03'
10°35'
10°40'
Thrust front
Thinned cont. crust
Oceanic crust
B
Italy
Mediterranean
Sea
A
Quaternary sediment
Miocene sediment
San Vincenzo rhyolites
Coquand and Ortaccio felsic dikes
Botro ai Marmi monzogranite pluton
Ligurian units:
Ophiolites and sedimentary cover
Tuscan Nappe:
Foredeep shales, sandstones
Limestones(a) and marble(b)
Ore deposits:
Fe-Cu-Zn-Pb(-Ag) skarn
Zn-Pb(-Ag) skarn
Sn-W-As ore

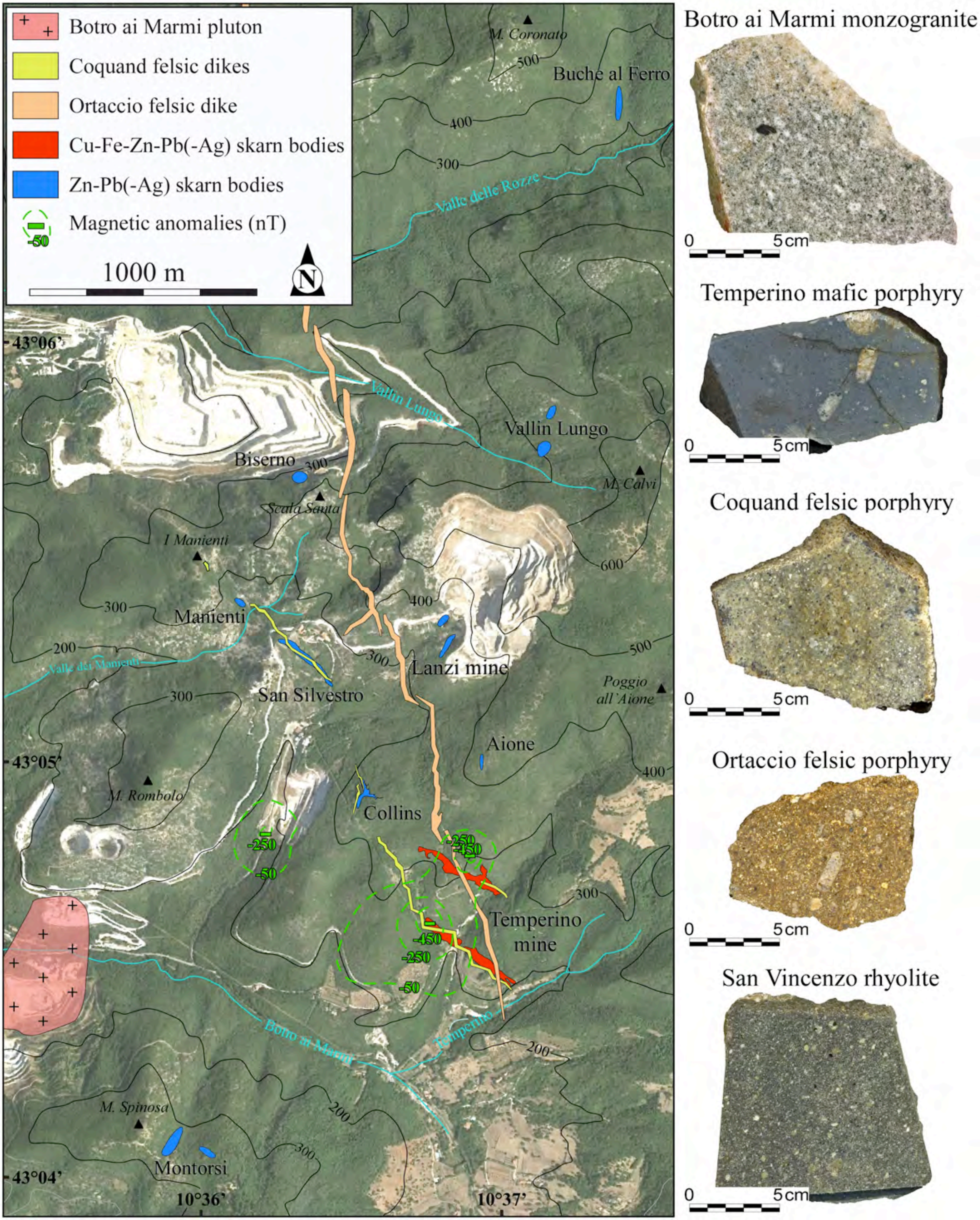
Botro ai Marmi pluton
Coquand felsic dikes
Ortaccio felsic dike
Cu-Fe-Zn-Pb(-Ag) skarn bodies
Zn-Pb(-Ag) skarn bodies
Magnetic anomalies (nT)
-50
1000 m
N
M. Coronato
500
Buche al Ferro
400
300
Valle delle Rozze
43°06'
Vallin Lungo
Vallin Lungo
Biserno
300
M. Calvi
Scala Santa
I Manienti
600
300
400
Manienti
200
Valle dei Manienti
300
Lanzi mine
500
300
San Silvestro
Poggio all'Aione
Aione
43°05'
M. Rombolo
400
Collins
-250
-50
-250
-450
300
Temperino mine
-450
-250
-50
Botro ai Marmi
Temperino
200
M. Spinosa
200
300
Montorsi
43°04'
10°36'
10°37'
Botro ai Marmi monzogranite
0
5 cm
Temperino mafic porphyry
0
5 cm
Coquand felsic porphyry
0
5 cm
Ortaccio felsic porphyry
0
5 cm
San Vincenzo rhyolite
0
5 cm

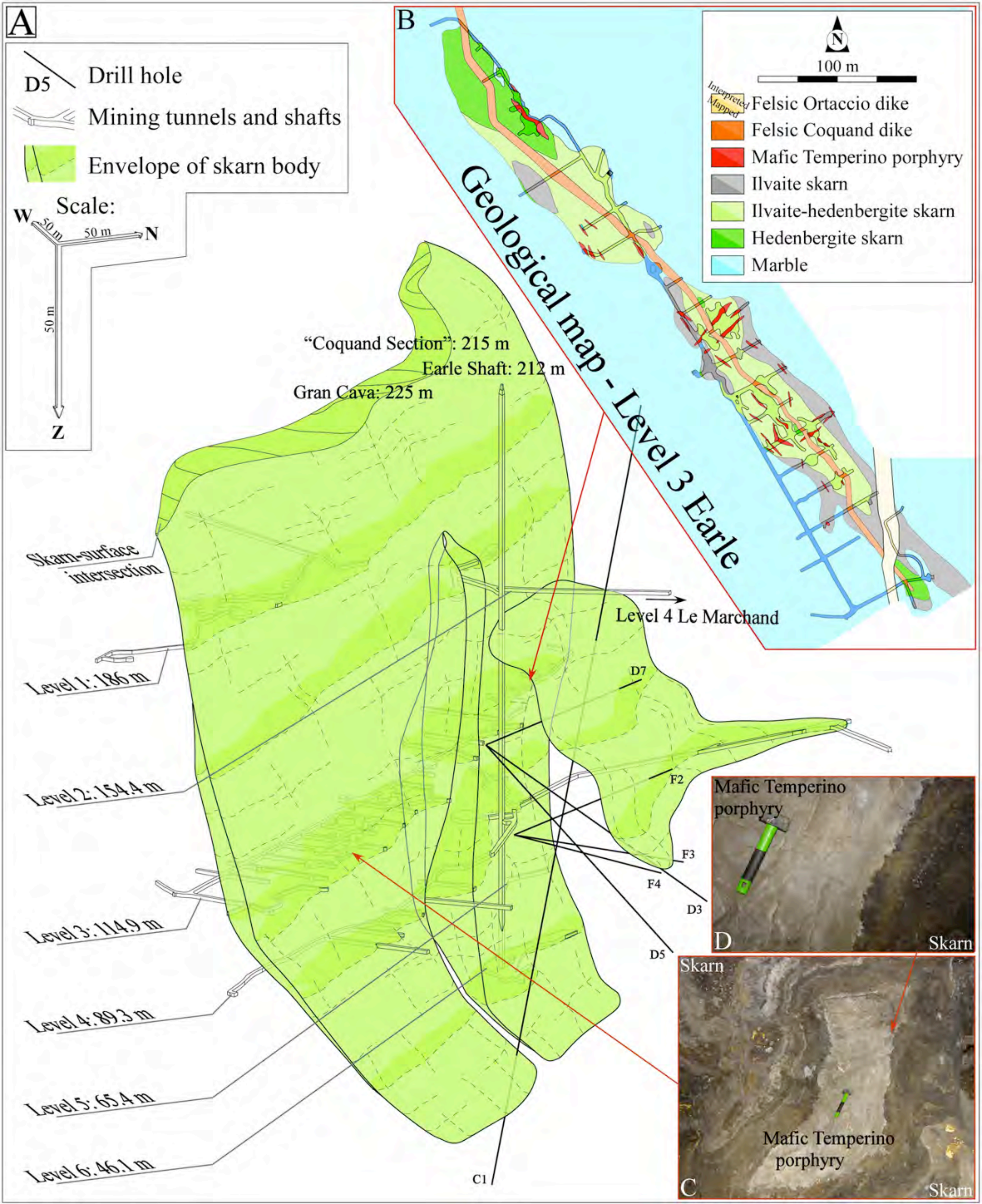
A
D5
Drill hole
Mining tunnels and shafts
Envelope of skarn body
Scale:
W
50 m
50 m
N
50 m
Z
"Coquand Section": 215 m
Earle Shaft: 212 m
Gran Cava: 225 m
Skarn-surface intersection
Level 1: 186 m
Level 2: 154.4 m
Level 3: 114.9 m
Level 4: 89.3 m
Level 5: 65.4 m
Level 6: 46.1 m
Level 4 Le Marchand
D7
F2
F3
F4
D3
D5
C1
B
100 m
Interpreted
Mapped
Felsic Ortaccio dike
Felsic Coquand dike
Mafic Temperino porphyry
Ilvaite skarn
Ilvaite-hedenbergite skarn
Hedenbergite skarn
Marble
Geological map - Level 3 Earle
Mafic Temperino porphyry
D
Skarn
Skarn
Mafic Temperino porphyry
C
Skarn

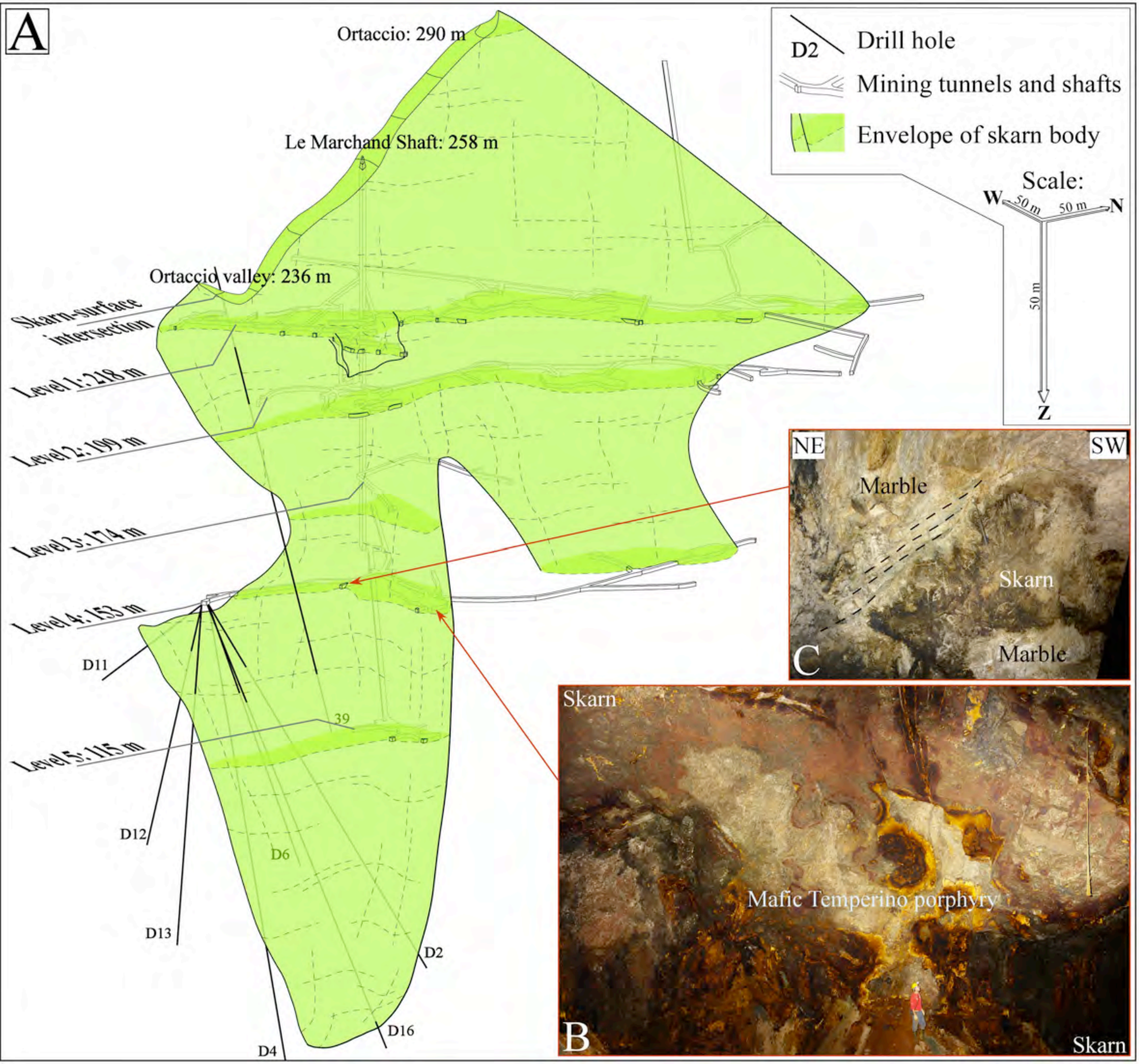

A
Ortaccio: 290 m
Le Marchand Shaft: 258 m
Ortaccio valley: 236 m
Skarn-surface intersection
Level 1: 218 m
Level 2: 199 m
Level 3: 174 m
Level 4: 153 m
Level 5: 115 m
39
D11
D12
D13
D6
D2
D16
D4
D2
Drill hole
Mining tunnels and shafts
Envelope of skarn body
Scale:
W
50 m
50 m
N
50 m
Z
NE
SW
Marble
Skarn
Marble
C
Skarn
Mafic Temperino porphyry
B
Skarn

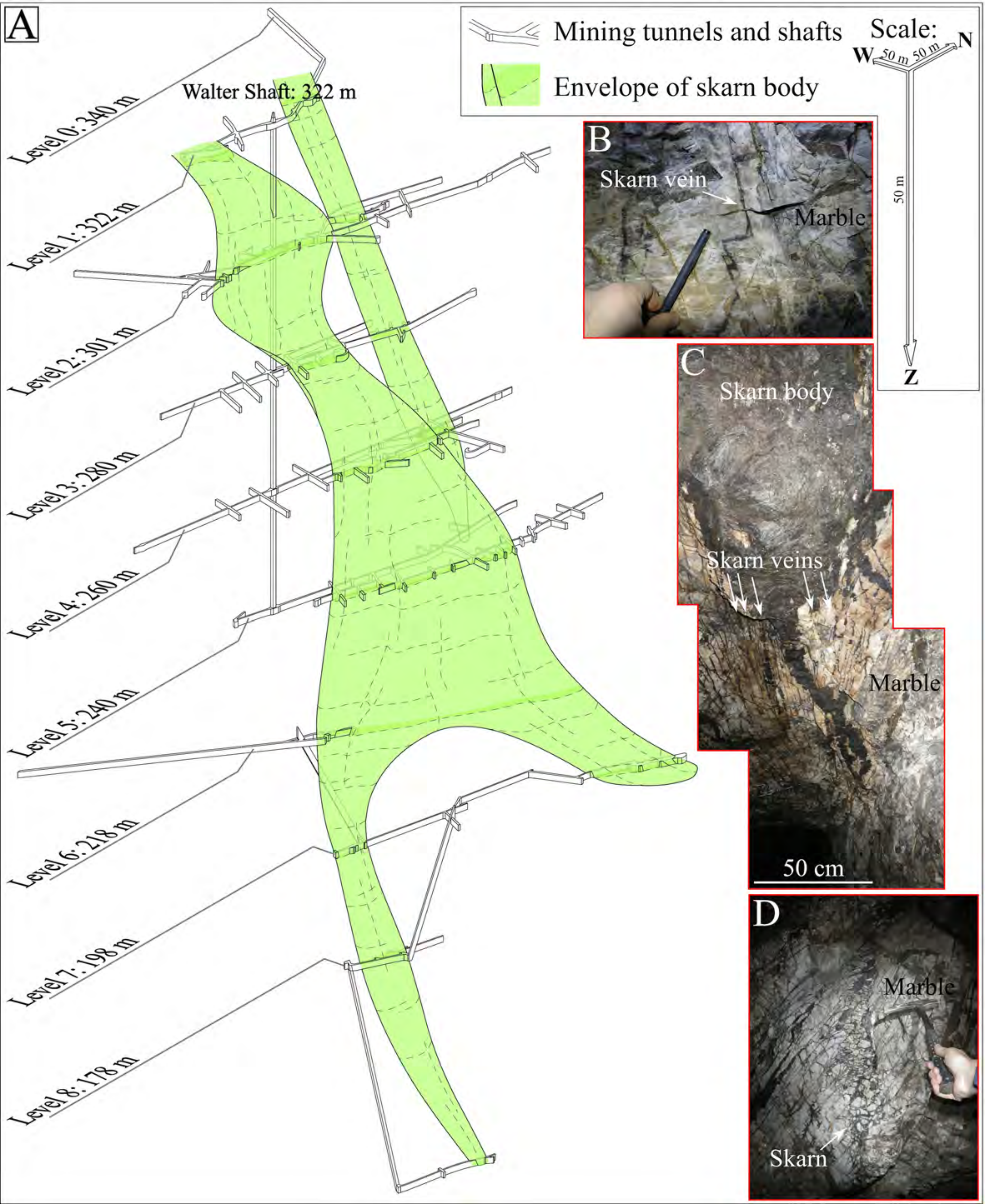

A
Mining tunnels and shafts
Envelope of skarn body
Scale:
W
50 m
50 m
N
50 m
Z
Walter Shaft: 322 m
Level 0: 340 m
Level 1: 322 m
Level 2: 301 m
Level 3: 280 m
Level 4: 260 m
Level 5: 240 m
Level 6: 218 m
Level 7: 198 m
Level 8: 178 m
B
Skarn vein
Marble
C
Skarn body
Skarn veins
Marble
50 cm
D
Marble
Skarn

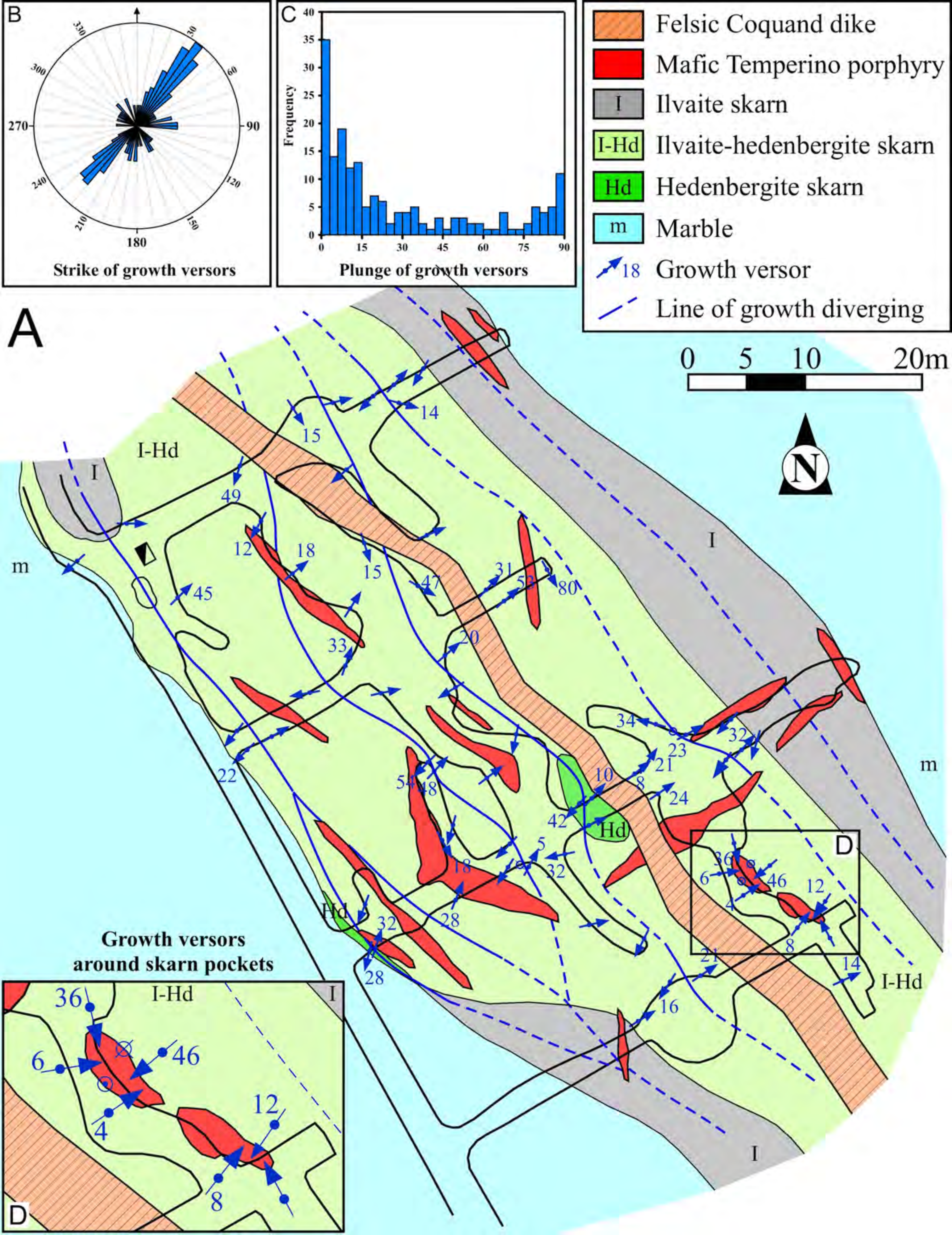
B
Strike of growth versors
C
Frequency
Plunge of growth versors
Felsic Coquand dike
Mafic Temperino porphyry
I
Ilvaite skarn
I-Hd
Ilvaite-hedenbergite skarn
Hd
Hedenbergite skarn
m
Marble
18
Growth versor
Line of growth diverging
A
0 5 10 20m
N
Growth versors around skarn pockets
D

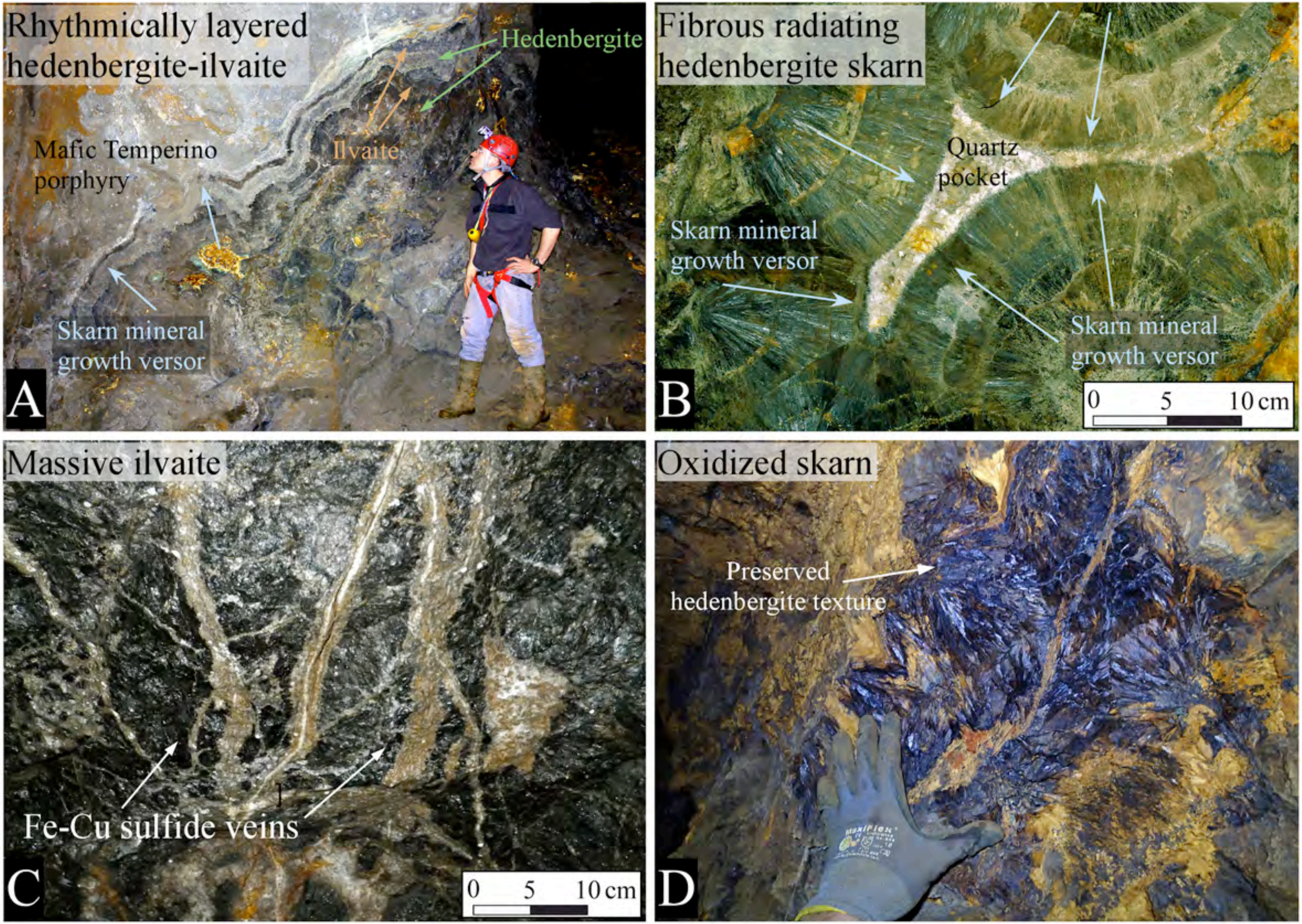
Rhythmically layered hedenbergite-ilvaite
Hedenbergite
Ilvaite
Mafic Temperino porphyry
Skarn mineral growth versor
A
Fibrous radiating hedenbergite skarn
Quartz pocket
Skarn mineral growth versor
Skarn mineral growth versor
0 5 10 cm
B
Massive ilvaite
Fe-Cu sulfide veins
0 5 10 cm
C
Oxidized skarn
Preserved hedenbergite texture
D

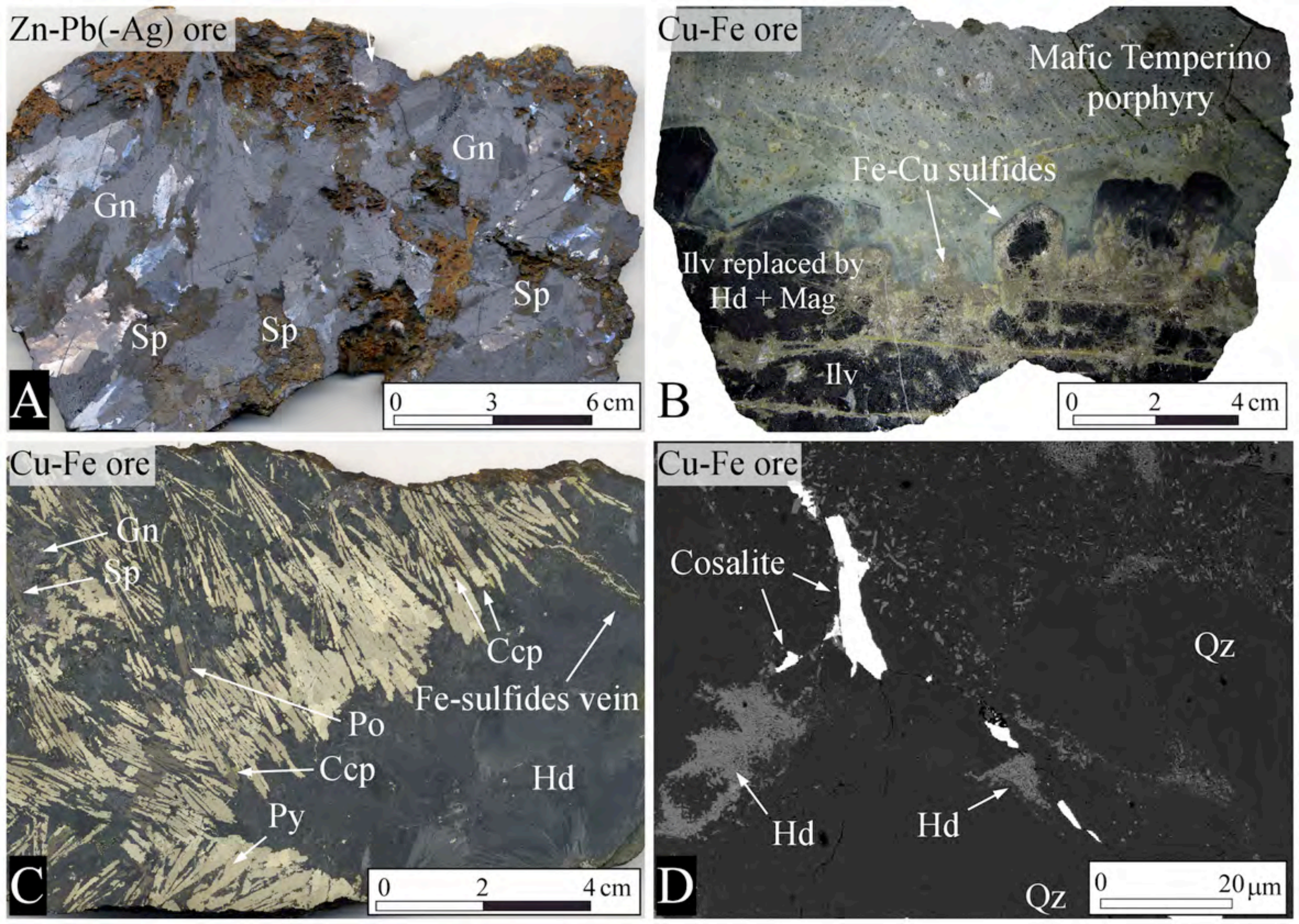
Zn-Pb(-Ag) ore
Gn
Gn
Sp
Sp
Sp
A
0 3 6 cm
Cu-Fe ore
Mafic Temperino porphyry
Fe-Cu sulfides
Ilv replaced by Hd + Mag
Ilv
B
0 2 4 cm
Cu-Fe ore
Gn
Sp
Ccp
Fe-sulfides vein
Po
Ccp
Hd
Py
C
0 2 4 cm
Cu-Fe ore
Cosalite
Qz
Hd
Hd
Qz
D
0 20 µm


A
Ilv
Qz + Cal
Gn
Sp
Hd
0
3 cm
B
Jhn
Gn
Sp
Gn
Sp
Jhn
Jhn
0
3 cm
C
Ccp
Py
Po
Ccp
Po
0
3 cm
D
Ilv
Hd
Py
Act
Adr
Ccp
0
3 cm
E
Gn crystal
Sp
Ccp
Sp
0
3 cm
F
Sp
Hd
Ccp
Gn
Hd
0
3 cm

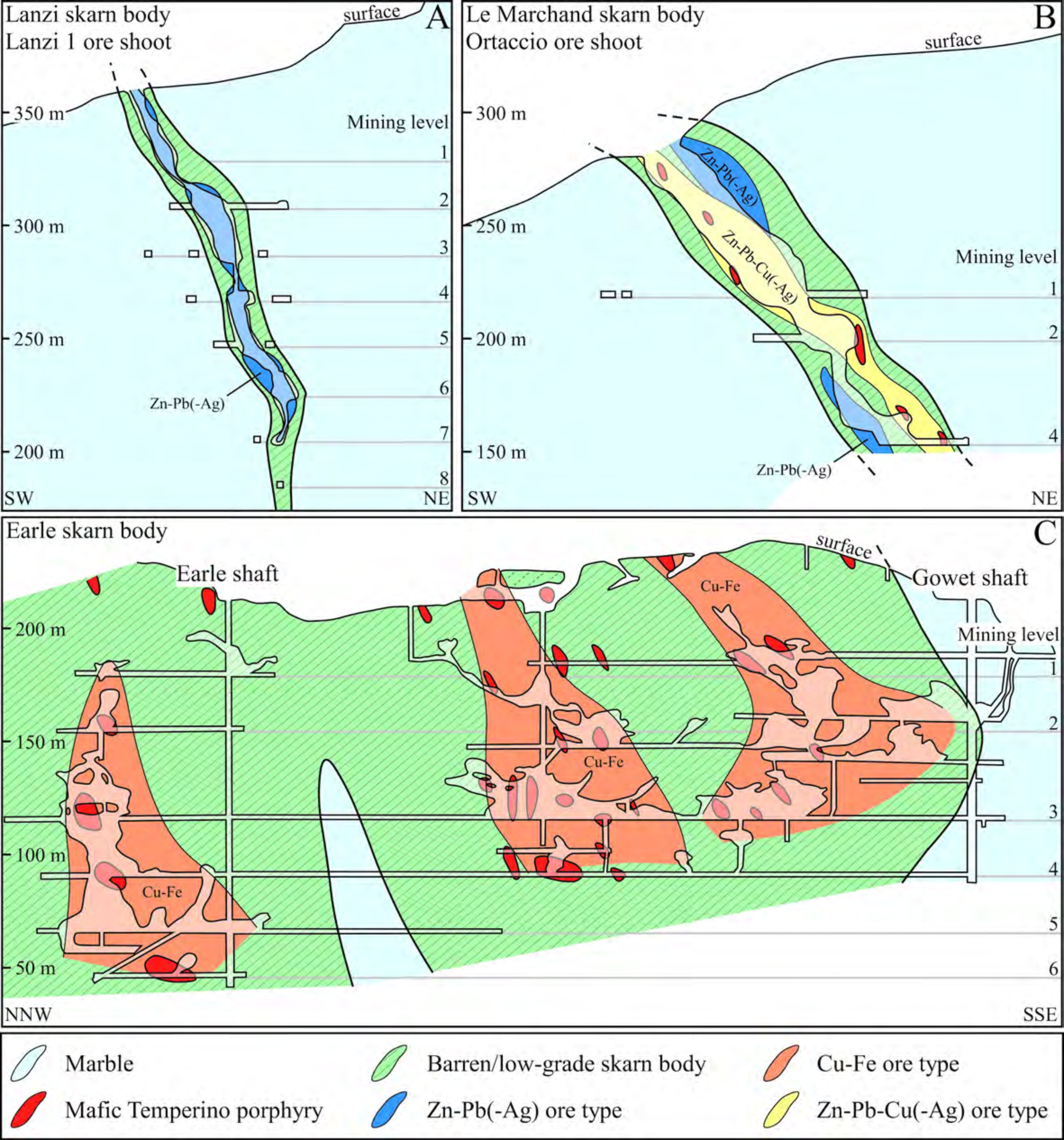

Lanzi skarn body
Lanzi 1 ore shoot
A
surface
350 m
300 m
250 m
200 m
Mining level
1
2
3
4
5
6
7
8
Zn-Pb(-Ag)
SW
NE
Le Marchand skarn body
Ortaccio ore shoot
B
surface
300 m
250 m
200 m
150 m
Zn-Pb(-Ag)
Zn-Pb-Cu(-Ag)
Mining level
1
2
4
Zn-Pb(-Ag)
SW
NE
Earle skarn body
C
Earle shaft
surface
Gowet shaft
Cu-Fe
Mining level
200 m
150 m
100 m
50 m
1
2
3
4
5
6
Cu-Fe
Cu-Fe
NNW
SSE
Marble
Barren/low-grade skarn body
Cu-Fe ore type
Mafic Temperino porphyry
Zn-Pb(-Ag) ore type
Zn-Pb-Cu(-Ag) ore type

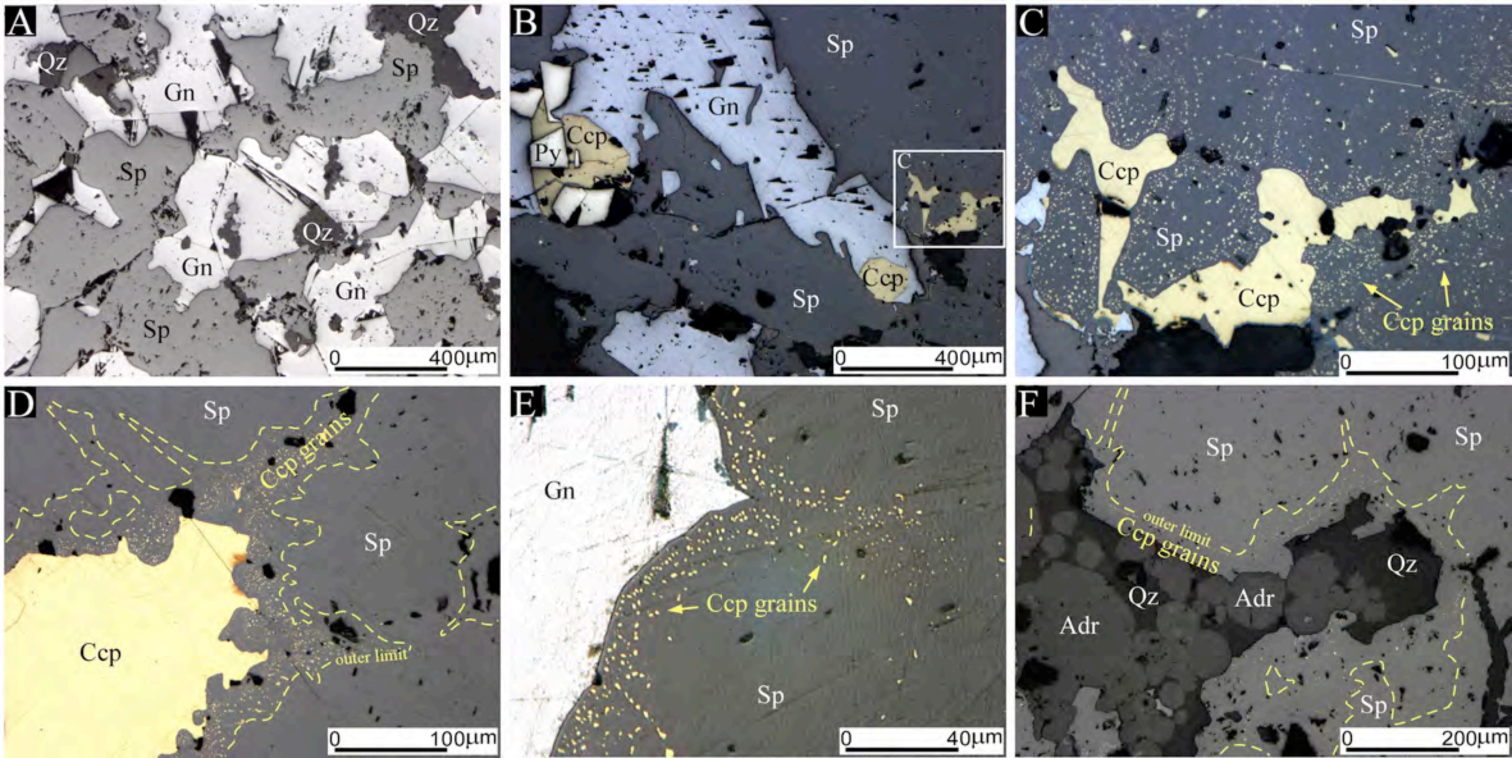
A
Qz
Qz
Sp
Gn
Sp
Qz
Gn
Gn
Sp
0 400µm
B
Sp
Gn
Ccp
Py
C
Ccp
Sp
0 400µm
C
Sp
Ccp
Sp
Ccp
Ccp grains
0 100µm
D
Sp
Ccp grains
Sp
Ccp
outer limit
0 100µm
E
Sp
Gn
Ccp grains
Sp
0 40µm
F
Sp
Sp
outer limit
Ccp grains
Qz
Qz
Adr
Adr
Sp
0 200µm

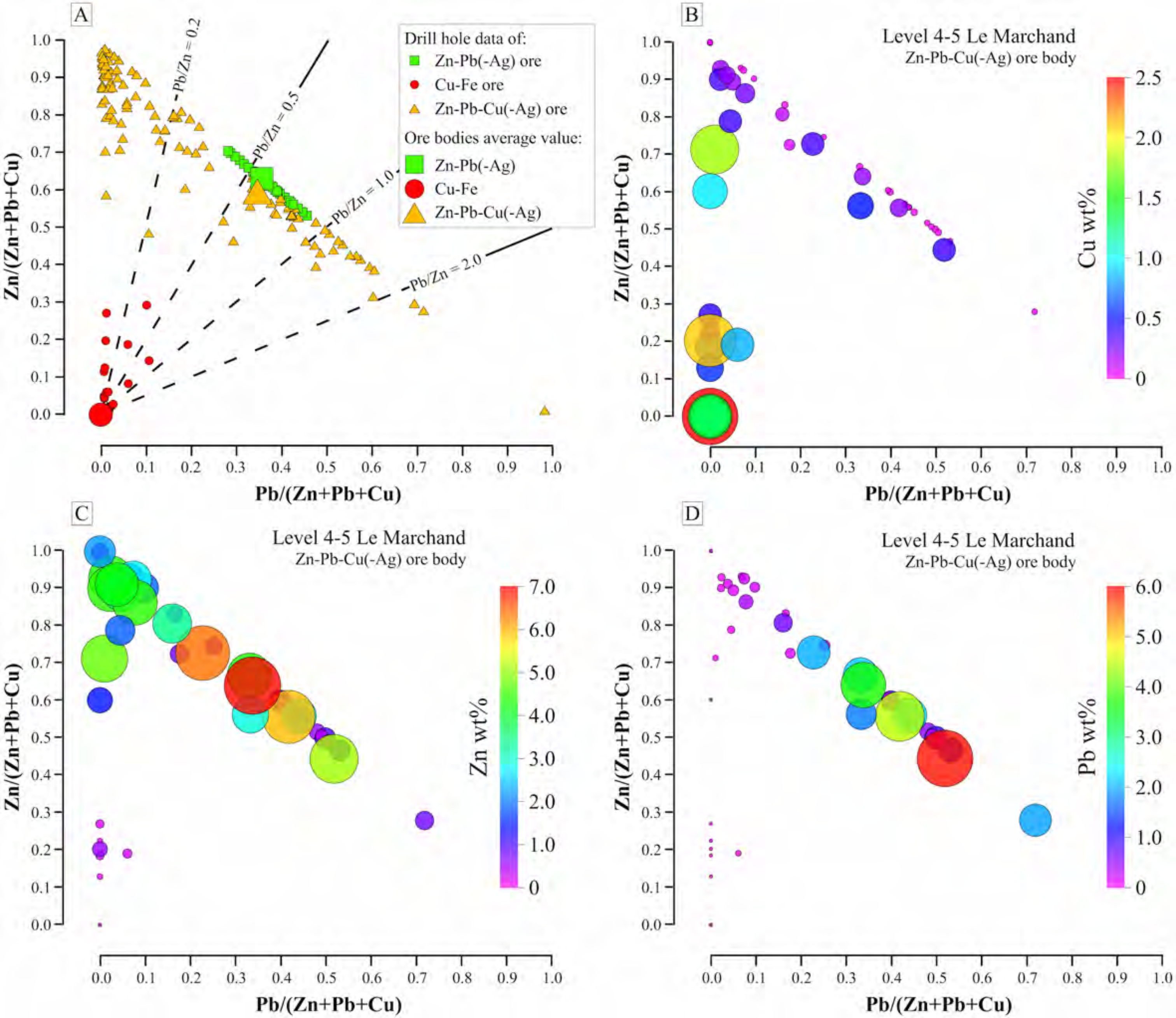

A
Drill hole data of:
Zn-Pb(-Ag) ore
Cu-Fe ore
Zn-Pb-Cu(-Ag) ore
Ore bodies average value:
Zn-Pb(-Ag)
Cu-Fe
Zn-Pb-Cu(-Ag)
Pb/Zn = 0.2
Pb/Zn = 0.5
Pb/Zn = 1.0
Pb/Zn = 2.0
Zn/(Zn+Pb+Cu)
Pb/(Zn+Pb+Cu)
B
Level 4-5 Le Marchand
Zn-Pb-Cu(-Ag) ore body
Cu wt%
C
Level 4-5 Le Marchand
Zn-Pb-Cu(-Ag) ore body
Zn wt%
D
Level 4-5 Le Marchand
Zn-Pb-Cu(-Ag) ore body
Pb wt%

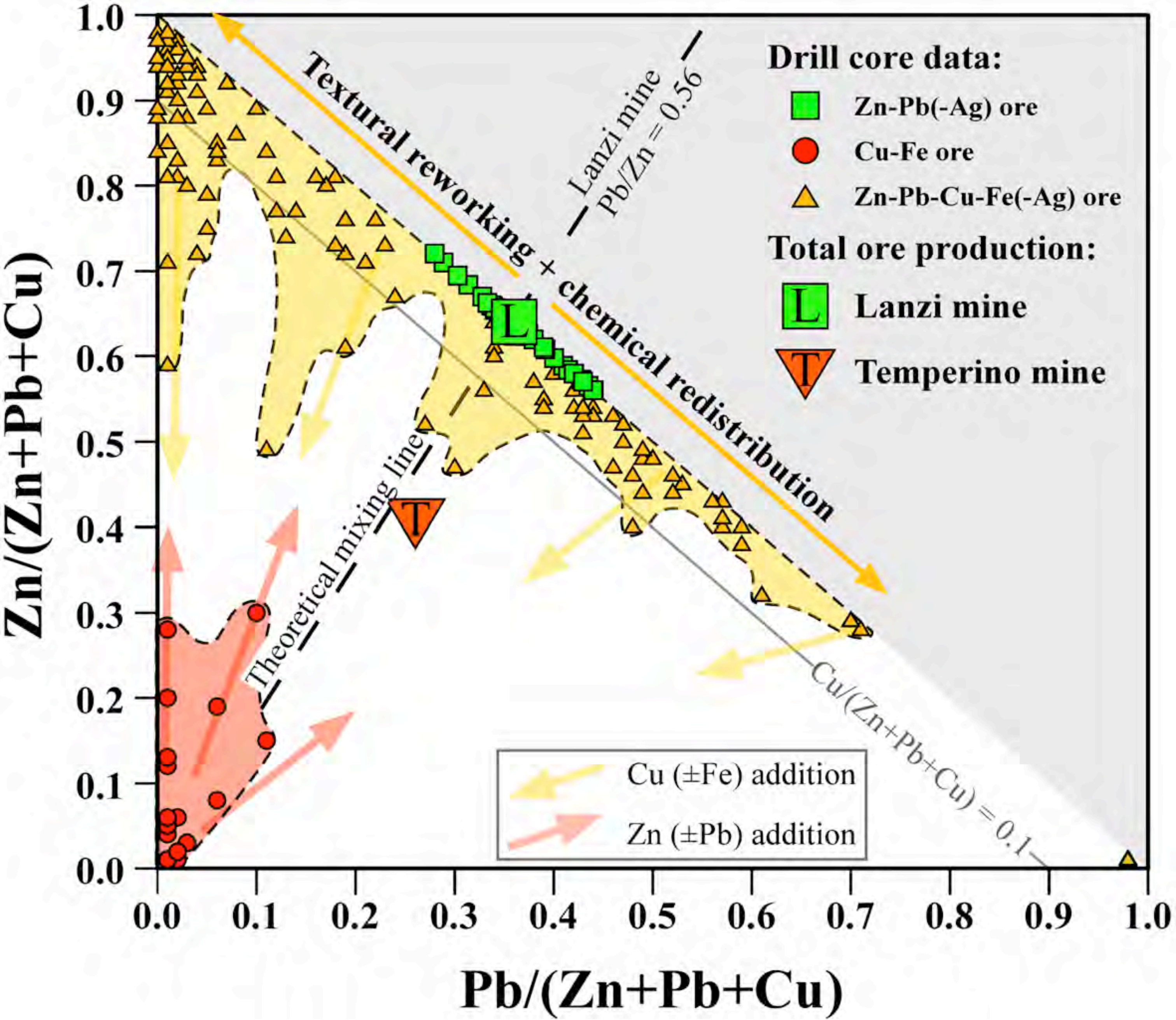

Drill core data:
Zn-Pb(-Ag) ore
Cu-Fe ore
Zn-Pb-Cu-Fe(-Ag) ore
Total ore production:
Lanzi mine
Temperino mine
L
T
Textural reworking + chemical redistribution
Lanzi mine
Pb/Zn = 0.56
Theoretical mixing line
Cu/(Zn+Pb+Cu) = 0.1
Cu (±Fe) addition
Zn (±Pb) addition
Zn/(Zn+Pb+Cu)
Pb/(Zn+Pb+Cu)
0.0
0.1
0.2
0.3
0.4
0.5
0.6
0.7
0.8
0.9
1.0

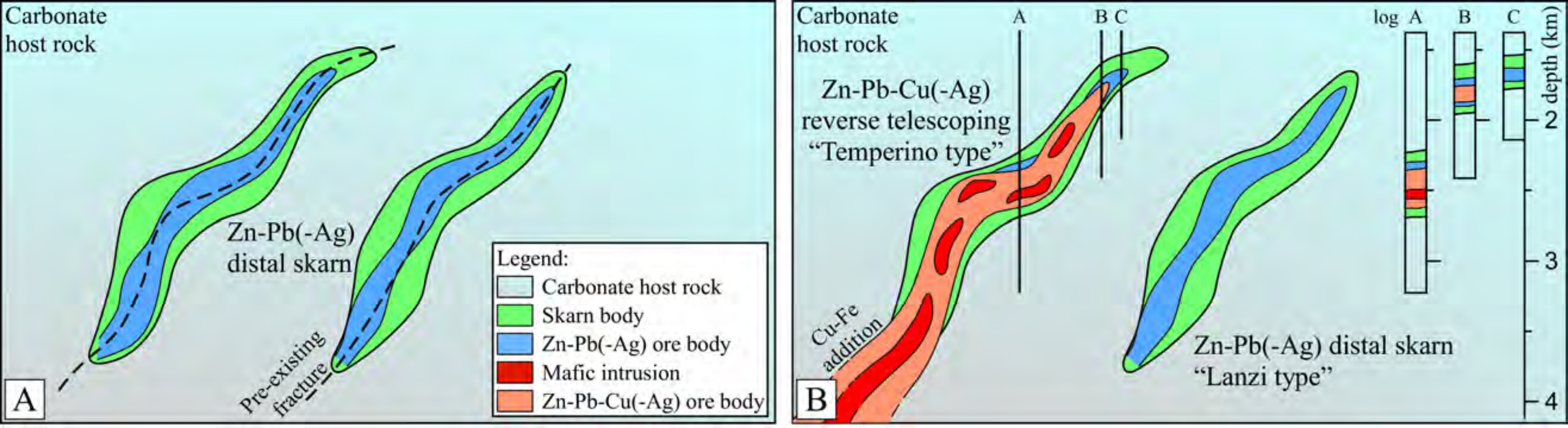

Carbonate host rock
Zn-Pb(-Ag) distal skarn
Pre-existing fracture
Legend:
Carbonate host rock
Skarn body
Zn-Pb(-Ag) ore body
Mafic intrusion
Zn-Pb-Cu(-Ag) ore body
A
Carbonate host rock
A
B
C
Zn-Pb-Cu(-Ag) reverse telescoping "Temperino type"
Cu-Fe addition
Zn-Pb(-Ag) distal skarn "Lanzi type"
log
A
B
C
depth (km)
2
3
4
B